



# Ozone Response to Emission Reductions in the Southeastern United States

Charles L. Blanchard<sup>1</sup>, George M. Hidy<sup>2</sup>

<sup>1</sup> Envair, Albany, CA, 94706, USA

5 <sup>2</sup> Envair/Aerochem, Placitas, NM, 87043, USA

*Correspondence to:* Charles L. Blanchard (cbenvair@pacbell.net)

**Abstract.** Ozone (O<sub>3</sub>) formation in the southeastern U.S. is studied in relation to nitrogen oxide (NO<sub>x</sub>) emissions using long-term (1990s – 2015) surface measurements of the Southeastern Aerosol Research and Characterization (SEARCH) network, U.S. Environmental Protection Agency (EPA) O<sub>3</sub> measurements, and EPA Clean Air Status and Trends Network (CASTNet) nitrate deposition data. CASTNet data show declining wet and dry nitrate deposition since the late 1990s, with total (wet plus dry) nitrate deposition fluxes decreasing linearly in proportion to reductions of NO<sub>x</sub> emissions in Alabama and Georgia. Annual nitrate deposition rates at Georgia and Alabama CastNet sites correspond to 30% of Georgia emission rates and 36% of Alabama emission rates, respectively. The fraction of NO<sub>x</sub> emissions lost to deposition has not changed over time. SEARCH and EPA CASTNet sites exhibit comparable downward trends in mean annual nitric acid (HNO<sub>3</sub>) concentrations. Mean annual total oxidized nitrogen (NO<sub>y</sub>) mixing ratios at SEARCH sites declined in proportion to NO<sub>x</sub> emission reductions. Annual 4<sup>th</sup>-highest daily peak 8-hour O<sub>3</sub> mixing ratios at EPA monitoring sites in Georgia, Alabama, and Mississippi exhibit statistically-significant ( $p < 0.0001$ ) linear correlations with annual NO<sub>x</sub> emissions in those states between 1996 and 2015. The annual 4<sup>th</sup>-highest daily peak 8-hour O<sub>3</sub> mixing ratios are declining toward non-zero values of ~45 – 50 ppbv. The O<sub>3</sub> declines are less than proportional to the decreases in NO<sub>x</sub> emissions: emissions decreased by ~60% and O<sub>3</sub> maxima declined ~30 – 35% at rates averaging ~1 ppbv y<sup>-1</sup>. Ozone production efficiency (OPE, molecules of O<sub>3</sub> produced per molecule of NO<sub>x</sub> oxidized) increased between 1999 and 2014, which affected the magnitude of the O<sub>3</sub> response to NO<sub>x</sub> emission reductions by partially offsetting precursor decreases and contributing to the nonlinear O<sub>3</sub> response. The results suggest increasing responsiveness of O<sub>3</sub> to NO<sub>x</sub>, but the effectiveness of ongoing NO<sub>x</sub> emission reductions will depend on the balance between changes in observed OPE and ambient NO<sub>x</sub> in the context of changes in anthropogenic emissions of volatile organic compounds (VOC).

## 25 1 Introduction

Ozone (O<sub>3</sub>) is a well-known and important product of photochemical processes in the troposphere involving nitric oxide (NO), nitrogen dioxide (NO<sub>2</sub>), and volatile organic compounds (VOCs). Ozone is of broad interest for its adverse effects on humans and ecosystems, as reflected by regulation through the U.S. Clean Air Act (e.g., U.S. EPA, 2014; 2015a).



Regulatory actions address extreme O<sub>3</sub> mixing ratios: the U.S. National Ambient Air Quality Standard (NAAQS), currently 70 ppbv, is applicable to the annual 4<sup>th</sup>-highest daily eight-hour maxima averaged over three year periods (U.S. EPA, 2015b; 2015c). By the early 1990s, U.S. emission control efforts began to focus on nitrogen oxides (NO<sub>x</sub> = NO + NO<sub>2</sub>) in addition to VOCs (NRC, 1991). O<sub>3</sub> management has generally relied on precursor reduction requirements estimated from models that  
5 integrate descriptions of non-linear chemical and atmospheric processes (e.g., Seigneur and Dennis, 2011), and guidance has also derived from so-called “observation-based” models linking O<sub>3</sub> and its precursors based on chemical reactions that are believed to drive ambient mixing ratios (e.g., NARSTO, 2000; Schere and Hidy, 2000).

Most of the work developing an observational basis for O<sub>3</sub>-precursor chemistry derives from field campaigns, sometimes focusing on urban conditions. Short-term data are available from aircraft flights, for example, or summer field measurements  
10 made at a variety of locations. Such studies usually are limited to a month or two of intense sampling. One example in the southern U.S. is the 1990 ROSE Experiment at Kinterbish, a rural, forested state park in western Alabama (Frost et al., 1998). This summer study of rural O<sub>3</sub> at low anthropogenic VOC and low NO<sub>x</sub> mixing ratios provided important insights into rural O<sub>3</sub> formation (Trainer et al., 2000). Other examples of short-term campaigns across the U.S. and elsewhere are reviewed in Solomon et al. (2000). More recent field studies include New England in 2002 (e.g., Griffin et al., 2004; Kleinman et al., 2007),  
15 Texas in 2006 (e.g., Berkowitz et al., 2005; Neuman et al., 2009), the mid-Atlantic region in 2011 (He et al., 2013), California in 2010 (Ryerson et al., 2013), Colorado in 2012 and 2014 (e.g., McDuffie et al., 2016), and the southeastern U.S. in 2013 (e.g., Neuman et al., 2016; Warneke et al., 2016). These campaigns and accompanying analyses of O<sub>3</sub> production and accumulation typically address summer, which historically has the strongest photochemical activity. However, strong photochemical O<sub>3</sub> production can occur under special circumstances in winter (e.g., Schnell et al., 2009).

Accounting for an O<sub>3</sub> background is important. O<sub>3</sub> background is associated with biogenic influence, large-scale transport, or the potential influence of the upper atmosphere (e.g., stratospheric intrusions, especially during spring) (e.g., Lin et al., 2012; Langford et al., 2015). The nature and magnitude of background O<sub>3</sub> remain an active area of research in the U.S. and Europe (Naja et al., 2003; Solberg et al., 2005; Ordóñez et al., 2007; Cristofanelli and Bonasoni, 2009; Arif and Abdullah, 2011; Zhang et al., 2011; Wilson et al., 2012). Hidy and Blanchard (2015) discuss definitions of continental and regional background  
25 O<sub>3</sub>. For this study, we adopt a definition of “background” that includes both the non-anthropogenic component and the eastern regional component.

Field studies have provided observational evidence of non-linearity in O<sub>3</sub>-NO<sub>x</sub> relationships (e.g., Trainer et al., 1993; Kleinman et al., 1994; Trainer et al., 1995; Hirsch et al., 1996; Frost et al., 1998; Kasibhatla et al., 1998; Nunnermacker et al., 1998; St. John et al., 1998; Sillman et al., 1998; Zaveri et al., 2003; Griffin et al., 2004; Travis et al., 2016). Long-term, post-  
30 1990s data are widely available for O<sub>3</sub> and NO<sub>2</sub> but detailed observations of total oxidized nitrogen (NO<sub>y</sub>) and VOC, and especially their component species, are typically lacking (e.g., Hidy and Blanchard, 2015). One of the longest records of urban and suburban data, comprising a series of short-term campaigns as well as continuous measurements, is from southern California. This region exemplifies a photochemically active urban regime. An analysis of multi-decadal (since the 1960s) data by Pollack et al. (2013) reveals how changes in atmospheric chemical reactions have contributed to the observed



reductions of O<sub>3</sub> in southern California since 1973. Long-term (more than one decade) measurements characterizing O<sub>3</sub> and NO<sub>y</sub> relationships in both urban and rural conditions are less common.

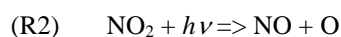
The photochemical regime in the Southeast represents humid subtropical conditions with urban emissions yielding elevated O<sub>3</sub> levels superimposed on a general regional background (Chameides and Cowling, 1995). The EPA O<sub>3</sub> and deposition data provide a regional basis for characterizing trends since the early 1980s (U.S. EPA 2016a; 2016b). In addition, the Southeastern Aerosol Research and Characterization (SEARCH) project (Hansen et al., 2003; Hidy et al., 2014) provides measurements that can be used to investigate changes in O<sub>3</sub> production resulting from changes in anthropogenic emissions in the southeastern U.S. The SEARCH network of eight sites began with the Southeastern Oxidant Study (SOS) (Chameides and Cowling, 1995; Meagher et al., 1998) rural locations, which were near (1) Centreville, AL, ~85 km southwest of Birmingham, (2) at Yorkville, GA, ~60 km northwest of Atlanta, GA and (3) at Oak Grove, MS, ~40 km southeast of Hattiesburg, MS, and 75 km north of Gulfport, MS, on private land within the confines of the Desoto National Forest (Hansen et al., 2003). Measurements of some gas-phase species began at these rural sites in 1992, thus providing a rural data record of over 20 years. Beginning in 1999, SEARCH added five sites in metropolitan Atlanta, GA, Birmingham, AL, Pensacola, FL, and Gulfport, MS.

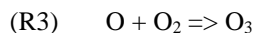
Our goal for this study is to extend earlier analyses of the photochemical response of O<sub>3</sub> to precursors through 2014, emphasizing relationships between O<sub>3</sub> and NO<sub>y</sub>. We first summarize relevant O<sub>3</sub> photochemistry to provide a context for the observational analysis. We then describe trends in emissions and ambient pollutant concentrations, and discuss O<sub>3</sub>, NO<sub>z</sub>, and HNO<sub>3</sub> observations at the SEARCH sites. Blanchard et al. (2014) previously explained the majority (66 - 80%) of the day-to-day variations in daily peak 8-hour average O<sub>3</sub> at SEARCH sites during March – October of 2002 - 2011 using meteorological variables coupled with ambient measurements of O<sub>3</sub> precursors (NO, NO<sub>2</sub>; limited measurements of VOCs) and NO<sub>x</sub> photochemical reaction products (NO<sub>z</sub>) and a statistical model (Blanchard et al., 2014). The previous analyses are extended here for data through 2014 to determine observed O<sub>3</sub> production efficiency (OPE). The analysis explains ongoing and potential future O<sub>3</sub> changes in relation to changes in ambient NO<sub>z</sub> and HNO<sub>3</sub> mixing ratios in the southeastern U.S.

## 2 Ozone-Nitrogen Oxide Chemistry

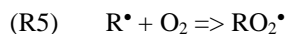
### 2.1 Key Atmospheric Reactions Linking O<sub>3</sub> with NO<sub>x</sub>

Net tropospheric O<sub>3</sub> accumulation occurs when sunlight acts on VOC and NO<sub>x</sub> emissions and the O<sub>3</sub> production rate exceeds O<sub>3</sub> loss (Trainer et al., 2000). Tropospheric O<sub>3</sub> mixing ratios are affected by solar intensity, chemical formation and loss (e.g., deposition) rates of O<sub>3</sub>, the rate of dispersion of O<sub>3</sub> and its precursors, meteorological factors, vertical entrainment and transport of plumes. NO<sub>2</sub> forms rapidly by reaction of NO with O<sub>3</sub> and photolysis of NO<sub>2</sub> produces O<sub>3</sub>, yielding steady-state mixing ratios of NO, NO<sub>2</sub>, and O<sub>3</sub> in the absence of other species as expressed by the photostationary state, or Leighton relationship (Seinfeld, 1986). The key reactions are (Seinfeld, 1986):





In the troposphere, NO<sub>2</sub> also forms by reaction of NO with peroxy (HO<sub>2</sub>) and alkyl peroxy (RO<sub>2</sub>) free radical species, which derive in turn from the reaction of VOCs with hydroxyl (HO), HO<sub>2</sub>, RO<sub>2</sub>, and alkyl radicals (Seinfeld, 1986). Radical production from VOCs creates a pathway for conversion of NO to NO<sub>2</sub> that does not consume O<sub>3</sub> (Atkinson, 2000), which then leads to higher O<sub>3</sub> mixing ratios. Key reactions are (Seinfeld, 1986):



(R8) HO<sup>•</sup> + NO<sub>2</sub> ⇒ HNO<sub>3</sub> O<sub>3</sub> accumulation is typically associated with high solar radiation intensity and temperatures favoring atmospheric reactions, lower wind speeds, and high anthropogenic emission rates (NARSTO, 2000). O<sub>3</sub> accumulation requires NO mixing ratios exceeding approximately 10 to 30 pptv (Atkinson, 2000; Logan, 1985), along with the presence of HO<sub>2</sub> and RO<sub>2</sub> radicals that react with NO to form NO<sub>2</sub>. The former conditions are normally met in urban air; NO<sub>x</sub> mixing ratios are much lower under typical conditions in rural southeastern areas, but still well above 30 pptv as reported in the U.S. (e.g., Hudman et al., 2007; Travis et al., 2016). Under these conditions, the O<sub>3</sub> photochemical production rate is proportional to the ambient NO multiplied by the sum of HO<sub>2</sub> and RO<sub>2</sub> radical mixing ratios, where the latter are weighted by their rates of reaction with NO (Trainer et al., 2000). Field studies show that observed rates of rural O<sub>3</sub> production are proportional to the rate of oxidation of NO<sub>x</sub>. Where VOCs are present for radical production and NO<sub>x</sub> is rate-limiting (Trainer et al., 2000), regional O<sub>3</sub> production can be expressed in terms of the derivative d[O<sub>3</sub>]/d[NO<sub>x</sub>], denoted the O<sub>3</sub> production efficiency (OPE) (Liu et al., 1987). OPE is understood as the number of molecules of O<sub>3</sub> formed per molecule of NO<sub>x</sub> oxidized and OPE increases as NO<sub>x</sub> mixing ratios decrease (Liu et al., 1987; Trainer et al., 2000). OPE reflects the mean number of NO-NO<sub>2</sub> cycles occurring, in which each photolysis of one NO<sub>2</sub> molecule generates one O<sub>3</sub> molecule until that NO<sub>2</sub> molecule is oxidized to nitric acid (HNO<sub>3</sub>) or to other species such as peroxyacetylnitrate (PAN). NO<sub>x</sub> reaction products, including HNO<sub>3</sub> and PAN, comprise NO<sub>z</sub>. For chemical reactions, the quantity d[O<sub>3</sub>]/d[NO<sub>z</sub>] is equivalent to d[O<sub>3</sub>]/d[NO<sub>x</sub>] but with opposite sign, and has therefore been used to estimate OPE; limitations due to emissions, transport, and deposition are discussed in Sections 4.3 and 4.4.

Empirically, the slope of a linear fit of afternoon O<sub>3</sub> (or O<sub>x</sub> = O<sub>3</sub> + NO<sub>2</sub>) versus NO<sub>z</sub> has been used to estimate OPE (e.g., Trainer et al., 1993; Pollack et al., 2013). This estimate is subject to certain limitations because it does not explicitly account for: (1) day-to-day variability in “old” (baseline or regional background) O<sub>3</sub> mixing ratios, (2) mixing of air masses having different emission histories, (3) rapid loss of HNO<sub>3</sub> (primarily through dry deposition, but also through gas-to-particle conversion) (Trainer et al., 2000), and (4) regeneration of NO<sub>2</sub> from PAN and certain other species. Because PAN regenerates NO<sub>2</sub>, it can serve as a reservoir rather than a true NO<sub>2</sub> sink (Singh and Hanst, 1981; Singh, 1987). In contrast, HNO<sub>3</sub> largely terminates the cycling between NO and NO<sub>2</sub>. Therefore, the relative yields of PAN and HNO<sub>3</sub> are of importance. Despite such limitations in using measurements to quantify OPE, data from field studies have been used since the 1990s to determine upper



bounds for OPE and the results have continued to appear in the literature as an indicator of relevance to O<sub>3</sub> chemistry (e.g., Berkowitz et al., 2005; Neuman et al., 2009; Kim et al., 2016). Investigators caution that field measurements reveal the net of production and loss, which potentially overestimates actual OPE by factors of 3 to 6 due to rapid chemical and deposition losses of HNO<sub>3</sub> and other NO<sub>z</sub> species (e.g., Trainer et al., 2000). Additional discussion of this ambiguity is found in Section 4.4.

Factors other than OPE are relevant to characterizing O<sub>3</sub> production and accumulation. In one case, OPE has not changed over time in southern California, but changes in the relative proportions of NO<sub>x</sub>-oxidation products have occurred and are thought to be instrumental in driving the rapid rates of O<sub>3</sub> decline in that area (Pollack et al., 2013). These results indicate that measurements of HNO<sub>3</sub> or PAN are needed to identify important changes in chemical pathways, considering not only OPE as defined by afternoon O<sub>3</sub>/NO<sub>z</sub> but also by using other indicators of O<sub>3</sub> production or accumulation, such as the O<sub>3</sub>/HNO<sub>3</sub> ratio.

## 2.2 National O<sub>3</sub> Response to Emission Reductions

Between 1980 and 2013, the national average of the annual 4<sup>th</sup>-highest peak daily 8-hour O<sub>3</sub> mixing ratios, a metric relevant to the U.S. O<sub>3</sub> NAAQS, declined by 33% (U.S. EPA, 2015d) as national VOC and NO<sub>x</sub> emissions decreased by 53% and 52%, respectively (U.S. EPA, 2015e). Across the U.S. and on multiple spatial scales from continental to urban, annual 4<sup>th</sup>-highest daily peak 8-hour O<sub>3</sub> mixing ratios between 1980 and 2013 show a statistically significant ( $p < 0.05$ ) linear fit to either annual average or to 98<sup>th</sup> percentile daily maximum hourly NO<sub>2</sub> mixing ratios; regression slopes are less than 1:1 and intercepts are in the range of 30 to 50 ppbv O<sub>3</sub> (Hidy and Blanchard, 2015). Proportionalities between O<sub>3</sub> and NO<sub>2</sub> that are less than 1:1 are expected, and the observed intercept terms are approximately consistent with typical O<sub>3</sub> mixing ratios of ~20 – 50 ppbv observed at remote monitoring sites (Oltmans et al., 2008; 2013; U.S. EPA, 2012; Fiore et al., 2014; Lefohn et al., 2010; 2014; Cooper et al., 2012; 2014).

Although nonlinearity of O<sub>3</sub> production and accumulation with respect to ambient VOC and NO<sub>x</sub> is well established (Lin et al., 1988), a tendency toward linearity is expected at sufficiently low NO<sub>x</sub> mixing ratios. As an example, the O<sub>3</sub> photochemical production rate during June 1990 at Kinterbish, AL was approximately linear over a range of ambient NO<sub>x</sub> from 0.1 to 2 ppbv (Trainer et al., 2000). Observed O<sub>3</sub> extrema can also exhibit an apparent linear or near-linear response to ambient NO<sub>x</sub> mixing ratios if the extrema consistently fall within the lower-right quadrant (NO<sub>x</sub>-sensitive regime) of an O<sub>3</sub>-VOC-NO<sub>x</sub> diagram, a concise graphical representation first established empirically from southern California data and later generated using the Empirical Kinetics Modeling Approach (EKMA) (illustrated in Hidy and Blanchard, 2015). The O<sub>3</sub>-VOC-NO<sub>x</sub> diagram has been adopted by many investigators for displaying the output of box models (e.g., Fujita et al., 2003; 2015) and grid-based photochemical models (e.g., Reynolds et al., 2003; 2004).

Southern California historically has exhibited the highest peak O<sub>3</sub> mixing ratios in the U.S. since the 1960s. Because of high ambient O<sub>3</sub> and precursor mixing ratios there and the complexity of the relationships of O<sub>3</sub> with NO<sub>x</sub> and VOC, some investigators have described southern California O<sub>3</sub> and precursor trends in terms of percentage changes. Pollack et al. (2013) report that peak 8-hour O<sub>3</sub> mixing ratios in southern California declined exponentially over time at a rate of 2.8% per year



between 1973 and 2010, thus decreasing O<sub>3</sub> levels by approximately a factor of three. This rate of O<sub>3</sub> decline exceeds rates occurring in other metropolitan areas (Hidy and Blanchard, 2015). O<sub>3</sub> extrema in southern California decreased along with declining mixing ratios of ambient VOCs and NO<sub>x</sub> (7.3% yr<sup>-1</sup> and 2.6% yr<sup>-1</sup>, respectively, 1960 – 2010) and declining ratios of VOC/NO<sub>x</sub> (4.8% yr<sup>-1</sup>) (Pollack et al., 2013). The rates of atmospheric oxidation of NO<sub>x</sub> increased over time and changes in  
5 NO<sub>x</sub> oxidation reactions increasingly favored production of HNO<sub>3</sub>, a NO<sub>x</sub> reaction product associated with radical termination and quenching of the O<sub>3</sub> formation cycle (Pollack et al. 2013). To our knowledge, changes in the relative proportions of atmospheric reaction products accounting for rapid rates of O<sub>3</sub> reduction have not been reported for locations other than southern California.

### 3 Methods

#### 10 3.1 Emissions and Ambient Air Quality Measurements

Air quality monitoring data were obtained from the EPA Air Quality System (AQS) data archives for all sites in Georgia, Alabama, and Mississippi (U.S. EPA, 2016a). Daily measurement values (i.e., peak daily 8-hour O<sub>3</sub> mixing ratio) as well as annual summary statistics (e.g., maxima, annual averages) were acquired. We obtained deposition data from the two EPA  
15 Clean Air Status and Trends Network (CASTNet) monitoring sites located within the study region: Sand Mountain, AL (125 km ENE of the SEARCH site at Centreville) and Georgia Station, GA (102 km SE of the SEARCH site at Yorkville) (U.S. EPA, 2016b).

Annual, state-level emission trends data were obtained from U.S. EPA (2016c; 2016d), Xing et al. (2013), and Hidy et al. (2014). Comparability of inventories is discussed in the supplementary material (Figure S1). Because the EPA trend inventory utilized different methods for estimating mobile source emissions prior to 2002 compared with 2002 and later years, we  
20 combined EPA trend estimates for 2002 – 2016 with the 1996 - 2001 emission estimates of Hidy et al. (2014), which are consistent with more recent EPA methods (supplementary material).

Hourly measurements of gases (NO, NO<sub>2</sub>, NO<sub>y</sub>, HNO<sub>3</sub>, and O<sub>3</sub>) were obtained from SEARCH public archives (Atmospheric Research and Analysis [ARA], 2017). All parameters measured at the sites are calibrated and audited to conventional reference standards, as described in ARA (2015). Network operations, sampling, and measurement methods are documented in Hansen  
25 et al. (2003; 2006); see also Table S1. The network consisted of eight extensively instrumented monitoring sites located in the southeastern U.S. along the Gulf of Mexico and inland (Figure S2): Pensacola, Florida (PNS) and Gulfport, Mississippi (GFP), urban coastal sites (~ 5 km and 1.5 km from the shoreline, respectively); Pensacola – outlying (aircraft) landing field (OLF) and Oak Grove, Mississippi (OAK), non-urban coastal sites near the Gulf (~20 km and 80 km inland, respectively); Atlanta, Georgia – Jefferson Street (JST) and North Birmingham, Alabama (BHM), urban inland sites; and Yorkville, Georgia (YRK)  
30 and Centreville, Alabama (CTR), non-urban inland sites. PNS, OAK, and GFP were closed at the end of 2009, 2010, and 2012, respectively. SEARCH site locations are described in detail, including discussion of possible emission influences, in Hansen et al. (2003) and Hidy et al. (2014). SEARCH VOC data are available for JST as daily data from 1999 through 2008, and U.S.





EPA VOC measurements are available for YRK as summer hourly data and as 24-hour samples collected every sixth day throughout the year (Blanchard et al., 2010). EPA VOC samples are also available for three other sites in the Atlanta area; only one of these additional sites reported data through 2014.

SEARCH meteorological parameters and gases are sampled at a height of 10 meters, characteristic of lower troposphere mixing ratios near the surface (Hansen et al., 2003; Hansen et al., 2006; Edgerton et al., 2007; Saylor et al., 2010). Gas and meteorological measurements commenced in 1992 at the rural sites of CTR, OAK, and YRK. The measurements at rural SEARCH sites included O<sub>3</sub>, NO, and NO<sub>y</sub> beginning in 1992, and NO<sub>2</sub> and HNO<sub>3</sub> measurements began in 1996. Consistent measurement methods have been utilized for all gases except NO<sub>2</sub>. NO<sub>2</sub> measurements commenced network-wide in 2002, and three NO<sub>2</sub> measurement methods have been employed during the network operations (Table S3). All three methods are NO<sub>2</sub>-specific, differing primarily in the light source used for photolysis of NO<sub>2</sub>. The NO<sub>2</sub> data exhibit consistency with NO and NO<sub>y</sub> measurements but with some variations occurring during specific years (e.g., 2001 and 2002, Figure S3). Because changes in NO<sub>2</sub> measurement methods could affect the computed NO<sub>z</sub> (NO<sub>y</sub> – NO – NO<sub>2</sub>), we repeat some data analyses using HNO<sub>3</sub> in place of NO<sub>z</sub>. As noted, HNO<sub>3</sub> data also provide useful insight into NO<sub>2</sub> termination reactions. HNO<sub>3</sub> measurements are the difference between NO<sub>y</sub> and denuded NO<sub>y</sub> (Table S1; Hansen et al., 2006).

Trace gas calibrations are done daily for O<sub>3</sub> and every third day for other gases. Reported detection limits (Table S1) are 0.05 – 0.1 ppbv for oxidized nitrogen species and 1 ppbv for O<sub>3</sub> (Hansen et al., 2003; 2006). NO<sub>2</sub> measurement uncertainties are estimated as ~30% prior to 2002 and ~10% after 2002 (Hansen et al., 2006). Measurement uncertainties are estimated to be 10% or less for other oxidized nitrogen species and 5% or less for ozone (2 sigma in all cases). Propagation of errors indicates corresponding 2-sigma measurement uncertainties averaging 0.5 ppbv for mid-afternoon NO<sub>z</sub> (< 0.1 ppbv for NO<sub>z</sub> < 1 ppbv) and 0.16 for the ratio NO<sub>z</sub>/NO<sub>y</sub>.

### 3.2 Data Analysis

Multiple methods were employed to characterize the variability of ambient O<sub>3</sub> and NO<sub>y</sub> mixing ratios. Analyses of seasonal variability used data from all months of each year. Diurnal hourly average mixing ratios were computed by year to characterize patterns of temporal change and to identify hours associated with O<sub>3</sub> maxima. Observed OPE was computed as previously done in measurement studies using afternoon O<sub>3</sub> and NO<sub>z</sub> data (Trainer et al., 1993; Kleinman et al., 1994; Trainer et al., 1995; Hirsch et al., 1996; Kasibhatla et al., 1998; Nunnermacker et al., 1998; St. John et al., 1998; Sillman et al., 1998; Zaveri et al., 2003; Griffin et al., 2004; Travis et al., 2016). Because past studies have examined O<sub>3</sub> formation in photochemically aged air (i.e., at locations distant from fresh emissions, where atmospheric reactions have acted on emissions from earlier times) during summers (e.g., Trainer et al., 1993), the analyses of summer OPE focus on the months of June and July to select weeks nearest maximum solar radiation (~ -20 days, + 40 days). Additional analyses of OPE were carried out for other months to facilitate comparisons across seasons. As for earlier studies, the calculations are based on afternoon times, using hourly values starting at 2 p.m. local standard time to represent the daily peak O<sub>3</sub> after morning production and before mixing ratios decline with decreasing photochemical reaction in later afternoon. In addition to characterizing O<sub>3</sub>/NO<sub>z</sub> and its change with time,



corresponding supporting analyses are presented for  $O_3/HNO_3$ . As a supplemental analysis, rates of maximum diurnal increase of  $O_3$  and  $HNO_3$  during late morning and early afternoon were computed for comparison of  $\Delta O_3$  with  $\Delta HNO_3$ .

## 4 Results

### 4.1 Trends

- 5 Hidy et al. (2014) report a 63% reduction of  $NO_x$  emissions in the southeastern US between 1996 and 2014. The largest  $NO_x$  emission changes in the Southeast occurred between 2007 and 2009 due to reductions of emissions from electric generating units (EGUs) and from diesel engine vehicles, and were accompanied by more gradual year-to-year reductions of gasoline-engine mobile-source  $NO_x$  emissions (de Gouw et al., 2014; Hidy et al., 2014).  $NO_x$  emission reductions led to approximately proportional responses of mean ambient  $NO_y$  and  $NO_z$  mixing ratios at SEARCH sites (Hidy et al., 2014).
- 10 The EPA CASTNet data show declining wet and dry nitrate deposition since the late 1990s, with total (wet plus dry) nitrate deposition fluxes decreasing linearly in proportion to reductions of  $NO_x$  emissions in Alabama and Georgia (Figure 1). Linear regression slopes indicate that the annual nitrate deposition fluxes at the Georgia and Alabama CASTNet sites correspond to 30% of Georgia emissions and 36% of Alabama emissions on an annual and statewide basis (Figure 1). Emissions are not spatially homogeneous and deposition losses likely vary with distance from emission sources. The two sites
- 15 are situated differently in relation to metropolitan areas, possibly affecting deposition fluxes; Sand Mountain (SND) is northeast of Birmingham and Georgia Station (GAS) is south of Atlanta. The linearity and statistical significance of the regressions indicates that the fraction of  $NO_x$  emissions lost to deposition has not changed over time (ratios of annual deposition-to-state-emissions varied without trend from 0.23 – 0.34 at GAS and 0.30 – 0.45 at SND). SEARCH and EPA CASTNet sites exhibit comparable downward trends in mean annual  $HNO_3$  concentrations (Figure S4).
- 20 Annual 4<sup>th</sup>-highest daily peak 8-hour  $O_3$  mixing ratios at compliance monitoring sites in Georgia, Alabama, and Mississippi exhibit statistically-significant ( $p < 0.0001$ ) linear correlations with annual  $NO_x$  emissions in those states between 1996 and 2015 (Figure 2), qualitatively consistent with past work indicating that high  $O_3$  would respond to reductions of  $NO_x$  emissions (Chameides and Cowling, 1995; Jacob et al., 1995; Kasibhatla et al., 1998). Spatial variability of the annual 4<sup>th</sup>-highest daily peak 8-hour  $O_3$  mixing ratios has decreased (Figure 2), consistent with an analysis of data from a larger number of U.S. and
- 25 European locations (Paoletti, et al., 2014). The annual 4<sup>th</sup>-highest daily peak 8-hour  $O_3$  mixing ratios are declining toward non-zero values, as indicated by the statistically-significant ( $p < 0.0001$ ) intercepts of ~45 – 50 ppbv (Figure 2). The  $O_3$  declines are less than proportional to the decreases in  $NO_x$  emissions, as indicated by the ~60% emission reduction and ~30 – 35%  $O_3$  declines shown in Figure 2, about equivalent to the national trends discussed in Section 2.2.
- SEARCH data are used to characterize the southeastern  $O_3$  response in detail. Between 1999 and 2014, the highest peak daily
- 30 8-hour  $O_3$  mixing ratios occurring each month (monthly  $O_3$  maxima) declined at all SEARCH sites at statistically significant ( $p < 0.01$ ) rates averaging ~1 ppbv  $y^{-1}$  (Figure 3). These trends are compared with emission changes in the Southeast, and with emission and  $O_3$  trends in southern California, in Table S2. The observed SEARCH  $O_3$  trends are consistent with other analyses





of North American observations (e.g., Chan, 2009; Lefohn et al., 2010; Paoletti, 2014; Simon et al., 2015) and with the trends occurring at EPA monitors in the Southeast (Figure 2). Both EPA (Figure 2) and SEARCH (Figure 3) data suggest that O<sub>3</sub> mixing ratios increased during the 1990s, then began declining. Specific aspects of the observed O<sub>3</sub> trends are discussed in Sections 4.2 through 4.4.

## 5 4.2 Seasonal Variations of O<sub>3</sub>, NO<sub>y</sub>, NO<sub>z</sub>, HNO<sub>3</sub>, and VOCs

The seasonal oscillations of monthly O<sub>3</sub> maxima in the Southeast are coupled to local or regional meteorology, solar radiation, and emissions (e.g., Blanchard et al., 2014; Hidy et al., 2014). The meteorological factors having the strongest influence on daily peak 8-hour O<sub>3</sub> mixing ratios at SEARCH sites are daily maximum temperature and mid-day relative humidity (RH), whose variations cause daily peak 8-hour O<sub>3</sub> mixing ratios to vary by ~ ±30 percent from mean peak 8-hour O<sub>3</sub> mixing ratios (Blanchard et al., 2014). Air mass back trajectories originating from the south (~ 150 to 200 degrees) exhibit peak 8-hour O<sub>3</sub> that is ~5 – 10 percent lower than average; daily peak O<sub>3</sub> decreases as 24-hour back trajectory distances increase from zero to ~600 km, consistent with association of higher O<sub>3</sub> concentrations with air mass stagnation rather than transport (Blanchard et al., 2014). At SEARCH sites, the monthly O<sub>3</sub> maxima (highest daily peak 8-hour O<sub>3</sub> each month) and mean daily peak 8-hour O<sub>3</sub> mixing ratios typically occurred in summer months, especially inland, and declined more than other monthly maxima (Figures 3 and 4). Summer means were not always higher than spring averages, especially at rural and coastal sites and during more recent years (Figure 4). Roughly constant winter monthly peak 8-hour maxima of ~40 ppbv occurred throughout the period of record (Figure 3). The seasonal variability of the highest peak daily 8-hour O<sub>3</sub> therefore declined over time (see also Table S3). Similar results were found for monthly means of hourly measurements, discussed in Section 4.3 on diurnal variations. Other recent studies have reported decreasing seasonal variability of O<sub>3</sub> across the U.S. using data from large numbers of monitoring sites (Chan, 2009; Chan and Vet, 2010; Cooper et al., 2012; Paoletti et al., 2014; Simon et al., 2015). Declines in seasonal variability are thought to result from changing rates of O<sub>3</sub> formation as precursor emissions have declined, or from increasing influence of intercontinental background O<sub>3</sub>, not from changes in seasonal variations of temperature and other meteorological factors (Chan, 2009; Cooper et al., 2012; Simon et al., 2015). With declining anthropogenic influence, background O<sub>3</sub> represents an increasingly important relative contribution. Background O<sub>3</sub> may also represent an increasing absolute contribution in our study area, as multiple studies have demonstrated increasing trends in global background O<sub>3</sub> mixing ratios (Ordóñez et al., 2007; Oltmans et al., 2008; Arif and Abdullah, 2011; Wilson et al., 2012).

Seasonal differences in mean mid-day (2 p.m.) hourly O<sub>3</sub> mixing ratios (selected to represent the average mid-point of the daily peak 8-hour O<sub>3</sub> maxima) are related in part to the extent of photochemical processing (Figure 5). At each site, the higher mean monthly 2 p.m. O<sub>3</sub> mixing ratios are associated with higher mean ratios of NO<sub>z</sub>/NO<sub>y</sub>. The lowest O<sub>3</sub> mixing ratios and ratios of NO<sub>z</sub>/NO<sub>y</sub> tend to occur during winter (December – February), with increasing values during other months. This result indicates that, on average, greater O<sub>3</sub> formation and accumulation occurs when a larger fraction of NO<sub>x</sub> has been converted to reaction products by early afternoon (Figure 5). At urban sites, mean NO<sub>z</sub>/NO<sub>y</sub> seldom exceeds ~0.6 due to ongoing emissions of NO<sub>x</sub>, which indicates that further O<sub>3</sub> formation and accumulation would be possible with additional daytime hours for



photochemical reactions to proceed. Similar results are obtained for comparison of mean 2 p.m. O<sub>3</sub> mixing ratios with mean ratios of HNO<sub>3</sub>/NO<sub>y</sub>. Additionally, higher mean monthly 2 p.m. O<sub>3</sub> mixing ratios are associated with higher mean mixing ratios of NO<sub>z</sub> and of HNO<sub>3</sub>.

The associations of O<sub>3</sub> with NO<sub>z</sub> found in the observations are indicative of NO<sub>x</sub>-oxidation reactions occurring in the presence of ambient VOCs, which provide a pool of free radical species that contribute to O<sub>3</sub> accumulation in both urban and rural areas. The effects of VOC species on O<sub>3</sub> formation depend on both their ambient concentrations and their reactivities. To describe VOC variations at sites with long-term VOC measurements, we use isoprene data as an indicator of biogenic VOCs and toluene as an indicator of anthropogenic VOCs (nominally emitted as a gasoline vapor). We also consider other reactive VOC species of interest, including  $\alpha$ -pinene (biogenic) as well as ethylene and xylenes (anthropogenic). Summer (June – August) months exhibit elevated ambient mixing ratios of rural and urban isoprene, typically about 5 – 10 ppbC, that are one to two orders of magnitude greater than those occurring between October and April (Figure 6). Transitions between low and high ambient isoprene mixing ratios occur in mid-May and mid-September in northern Georgia (Figure 6). Annual mean isoprene mixing ratios were relatively constant, ~2.5 – 3 ppbC, between 1998 and 2014. OH reactivity, computed as the product of concentration and k<sub>OH</sub>, indicates that biogenic VOCs, primarily isoprene, represent ~20% of the VOC reactivity at JST, ~30% at South Dekalb (SDK, located in metropolitan Atlanta ~16 km southeast of JST), and ~50% at YRK, averaged over all samples collected between 1999 and 2007 (Blanchard et al., 2010a). Isoprene OH reactivity predominates at JST in summer but not in spring or fall (Figure 6). Through precursor interactions, seasonal variations in isoprene mixing ratios are expected to affect seasonal variations in O<sub>3</sub> mixing ratios and production rates.

Alkenes and aromatic compounds (largely originating from motor vehicle and industrial process emissions) account, respectively, for ~20 – 40% and ~20% - 25% of the average VOC OH reactivity at JST, SDK, and YRK (Blanchard et al., 2010a). Mean mixing ratios of ethylene and aromatic compounds vary substantially between urban and rural sites and exhibit less, and a different, seasonal variation than does isoprene, peaking in the fall rather than in the summer (Figures 6, S5, S6). Daily average mixing ratios of toluene, xylenes, and ethylene decline over the years, consistent with regulatory reductions of anthropogenic VOC emissions (Figures S5, S6). Seasonal variations in ambient mixing ratios and trends in the anthropogenic emissions of aromatic compounds are expected to influence O<sub>3</sub> mixing ratios and production in urban settings (rural anthropogenic VOC mixing ratios are lower but detectable).

The 24-hour average VOC mixing ratios are of somewhat limited value for showing the influence of VOCs on O<sub>3</sub> formation and accumulation. VOC influence is dependent on NO<sub>x</sub> mixing ratios, which vary depending on proximity to emission sources and time of day. Meteorological variability, including diurnal and day-to-day changes in temperature, vertical mixing, cloud cover, photolysis, and air mass transport, further obscures the quantitative effects of VOCs on seasonal and interannual variations of O<sub>3</sub>. Influences of anthropogenic VOCs at SEARCH sites have previously been reported (Blanchard et al., 2010b; 2014) and are not analyzed beyond this summary.



### 4.3 Diurnal Variations of O<sub>3</sub>, NO<sub>y</sub>, NO<sub>z</sub>, and HNO<sub>3</sub>

Summer (June – August) mean O<sub>3</sub> mixing ratios exhibit characteristic nocturnal minima and mid-day (noon to 4 p.m., midpoint ~ 2 p.m.) maxima at all SEARCH sites (Figure 7). This diurnal pattern remained essentially the same at both the urban and rural sites from 1999 through 2014, but the daytime maxima decreased. Between 1999 and 2014, the summer mean mid-day maxima declined by ~30 ppbv at all sites, while nocturnal means exhibited variable responses (Figure 7). Similar diurnal variations occur throughout the year, with smaller decreases in the mean mid-day O<sub>3</sub> maxima occurring during seasons other than summer (Figures S7 – S9). By the end of the study period, diurnal O<sub>3</sub> profiles were higher during spring (March through May) than summer at the rural sites (CTR and YRK, Figures S7 and S8), consistent with the reduction in summer mean monthly daily peak 8-hour O<sub>3</sub> averages (Figure 4). Decreasing summer diurnal mean NO<sub>y</sub>, HNO<sub>3</sub>, and NO<sub>z</sub> mixing ratios were also observed, with a general flattening of the profiles and with the times of maxima remaining consistent (Figures S10-12). O<sub>3</sub> changes are discussed in relation to changes in NO<sub>y</sub> and NO<sub>z</sub> in Section 4.4, with emphasis on summer and additional consideration of spring months.

### 4.4 Observed Ozone Production Efficiency (OPE)

#### 4.4.1 Linear Models

Over the range of ambient mixing ratios observed across 15 years, the June-July 2 p.m. O<sub>3</sub> values are distinctly nonlinear in relation to ambient NO<sub>z</sub> and HNO<sub>3</sub> mixing ratios (Figure 8). More variability is evident at urban sites than at rural sites, consistent with variable influence of urban NO<sub>x</sub> and perhaps VOC emissions on O<sub>3</sub>. We employ multiple approaches to account for nonlinearity and variability in using the data to estimate observed OPE. We use “observed” to distinguish between field data-based values and theoretically-based values. The former are affected by an ambiguity associated with deposition losses, discussed below.

Linear regressions are fit to the afternoon data by year, as shown in Figure 9 for 2013 and in Table S4 for all years. During multi-week periods within any summer, all sites exhibit near-linear relationships of mid-day O<sub>3</sub> to NO<sub>z</sub>. Because the ranges of NO<sub>x</sub> and NO<sub>z</sub> mixing ratios within each year are limited, year-specific relationships are close to linear and linear models are statistically significant. We use the slopes of the linear regressions of O<sub>3</sub> vs. NO<sub>z</sub> as one set of estimates of year-specific and site-specific observed OPE. Figure 9 indicates that either more O<sub>3</sub> molecules formed per molecule of NO<sub>x</sub> consumed in rural locales than in urban areas, or that greater losses of NO<sub>z</sub> occurred at the rural sites as discussed below. At all sites, similar results are obtained for regressions of O<sub>x</sub> (O<sub>3</sub> + NO<sub>2</sub>) vs NO<sub>z</sub> compared with O<sub>3</sub> vs NO<sub>z</sub> (Figure 9, caption). At 2 p.m., rural O<sub>3</sub> mixing ratios are nearly identical with O<sub>x</sub> mixing ratios and with other metrics (e.g., O<sub>3</sub> – [NO<sub>y</sub> – NO]) (Figure S13). At urban sites, 2 p.m. NO<sub>2</sub> mixing ratios are non-negligible, but this difference alters the intercepts rather than the slopes of the regressions of O<sub>x</sub> vs NO<sub>z</sub> compared with O<sub>3</sub> vs NO<sub>z</sub> (Figure 9).

Plotting the year-specific (June – July) computed observed OPE (regression slopes) versus mean June – July 2 p.m. NO<sub>z</sub> shows that OPE has increased as ambient NO<sub>z</sub> mixing ratios have decreased, subject to year-to-year variability (Figure 10, Table S4).



Similar urban-rural differences and patterns of increasing OPE are also observed when data are restricted to March and April (spring) at YRK and JST (Figure S14). The results for spring show more variability than the summer year-specific linear models, but nonetheless indicate that in spring fewer O<sub>3</sub> molecules formed per molecule of NO<sub>x</sub> consumed compared to summer. One key difference between spring and summer days is that cumulative solar radiation between sunrise and 2 p.m. is greater on summer days than on spring days, presumably fostering greater photochemical extent of reaction and accumulation of O<sub>3</sub> during summer.

The regression slopes determined from 2 p.m. data could be biased high as estimates of observed OPE if background O<sub>3</sub> is consistently higher on high-O<sub>3</sub> days than on low-O<sub>3</sub> days and NO<sub>z</sub> is not (random variations in day-to-day background O<sub>3</sub> and NO<sub>z</sub> would, in contrast, introduce variations, or scatter, around the regression lines). We checked for potential bias of this type by repeating the analyses using differences in mixing ratios. Two sets of difference-based regressions are used: (1) the differences between 2 p.m. and 10 a.m. hourly measurements, and (2) the differences between 11 a.m. and 10 a.m. hourly measurements. The differences are computed for each day to minimize or eliminate the unknown day-specific background levels, and are then used in the regressions. These hours were selected to focus on times of day when the atmosphere is well-mixed. The morning rise in mixing heights is expected to contribute to increases in the mixing ratios of secondary species as aged air aloft is incorporated into the mixed layer. The most rapid rates of increase in diurnally-averaged O<sub>3</sub>, NO<sub>z</sub>, and HNO<sub>3</sub> values occur between ~8 a.m. and 12 noon local time (Figures 7, S8 – S9). By mid- to late-morning hours during summer, considerable vertical entrainment has occurred, and subsequent changes in the mixing ratios of secondary species likely reflect same-day atmospheric chemical reactions. Computing afternoon – morning differences and late morning – mid-morning differences helps account for day-to-day variations in regional background O<sub>3</sub>, but also introduces higher relative uncertainties because four measurements (two differences) are used in the regressions. Results for all three approaches are tabulated in Table S5, by site and year. Like the regressions based on 2 p.m. measurements, the difference-based regressions indicate that observed OPE has increased over time (Table S5, Figures S15 – 17). The best statistical fits are for the regressions using non-differenced afternoon data. The difference-based regressions exhibit lower slopes than the non-differenced afternoon regressions, which could be due to lesser statistical fit, or to better accounting for regional background O<sub>3</sub>, or to a combination of these factors. The difference-based regressions suggest that the observed OPE increased from less than 5:1 in the late 1990s and early 2000s to values between 5:1 and 10:1 after 2010 (Figures S15 – S17; Table S5). These values are consistent with previous results in which observed OPE was determined while accounting for day-to-day variations in meteorology, which indicated that within the range of 1 to 5 ppbv NO<sub>z</sub>, JST, YRK, and CTR O<sub>3</sub>/NO<sub>z</sub> slopes were 3.5, 5.0, and 7.1, respectively, for measurements made during March – October of 2002 - 2011 (Blanchard et al., 2014).

A second potential bias could result from changes in NO<sub>2</sub> measurement methods, previously described; this possibility was checked by using regressions of O<sub>3</sub> vs. HNO<sub>3</sub> (Figure S18). The results indicate that the relationship in Figure 10 is not an artifact of changes in NO<sub>2</sub> measurement methods. The record is more complete for the regressions of O<sub>3</sub> vs. HNO<sub>3</sub>, because the HNO<sub>3</sub> measurements were made over a longer time than the NO<sub>2</sub> measurements (and the latter are needed for computing NO<sub>z</sub>). As shown for YRK, the year-specific slopes of 2 p.m. O<sub>3</sub> vs. NO<sub>z</sub> and for O<sub>3</sub> vs. HNO<sub>3</sub> each increased substantially after



about 2008 (Figures 10, S18). The  $O_3$  vs.  $NO_2$  and  $O_3$  vs.  $HNO_3$  regression slopes tend to level out after 2011, and possibly decrease somewhat, but variability is too high to project beyond the observed data ranges (Figures 10, S18). Similar results are obtained for spring for JST and YRK (Figures S19 and S20).

In Figure 9, the intercepts of year-specific regressions for 2013 approach 20 ppbv  $O_3$ , which could be interpreted as a regional background  $O_3$  level relatively unaffected by local chemistry. These values are lower than estimated western regional background  $O_3$  levels of  $\sim 40 - 50$  ppbv (Lefohn et al., 2014; Dolwick et al., 2015) but are consistent with estimates of background  $O_3$  less than  $\sim 30$  ppbv in Atlanta (Lefohn et al., 2014). The intercept terms for earlier years are higher than for later years; for example, the intercepts for the YRK regressions range from  $27 \pm 3$  to  $42 \pm 4$  ppbv prior to 2009 (for all but two of these years, intercepts are  $36 - 38$  ppbv). The intercept terms for earlier years are consistent with 1997 – 2006 eastern U.S. summer baseline  $O_3$  levels ( $32 \pm 12$  ppbv) reported by Chan and Vet (2010). Higher intercepts are associated with lower OPE, and could be due to fitting a linear regression to the mid-range of the nonlinear relationship between  $O_3$  and  $NO_2$ , as shown in Figure 8. Alternatively, the trend toward lower intercepts could reflect declining mixing ratios upwind of the study sites, consistent with documented long-term reductions of ambient  $O_3$  mixing ratios throughout the U.S. (e.g., Chan and Vet, 2010; Lefohn et al., 2010; Paoletti, 2014; Simon et al., 2015; Hidy and Blanchard, 2015).

As discussed next, previous studies obtained lower OPE values after adjusting for deposition losses. While such corrections could be applied to our observed OPE values, we instead ask whether our apparent increase in observed OPE could be due to increasing losses of  $NO_2$  species, especially  $HNO_3$ , over the long-term SEARCH record, rather than to increasing production efficiency. As previously noted, however, the CASTNet data show declining rates of both wet and dry nitrate deposition since the late 1990s, with no change in the ratio of deposition to emissions (Figure 1). Therefore, the long-term increase in observed OPE cannot be attributed to increasing deposition losses of  $HNO_3$  (whether absolute or fractional). Qualitatively, the CASTNet data suggest that the observed OPEs would likely be at least a factor of two smaller if adjusted for deposition losses. This adjustment would be comparable to the 1990s studies discussed below, which yielded unadjusted OPEs of  $\sim 5:1$  to  $11:1$  compared with OPEs of  $\sim 3:1$  to  $5:1$  when adjusted for deposition.

#### 4.4.2 Comparisons with Observed and Modeled OPE

The SEARCH observed afternoon OPE values of  $\sim 5:1$  prior to 2003 – 2007 are comparable to, or lower than, similar regression results obtained in studies during the 1990s, which showed observed summer OPE values of  $11:1$  in rural Georgia in 1991 (Kleinman et al., 1994),  $8.5:1$  at rural eastern sites (Trainer et al., 1993),  $7:1$  near Birmingham, AL in 1992 (Trainer et al., 1995),  $5.7:1$  near Nashville, TN in 1995 (Sillman et al., 1998), and  $4.7:1$  near Nashville, TN, in 1999 (Zaveri et al., 2003), and to modeling results and observations with composite OPE values of 6.7 and 7.6, respectively, within the afternoon planetary boundary layer in the eastern U.S. during the summer of 2002 (Godowitch et al., 2011) The SEARCH regression OPE values prior to 2003 – 2007 are higher than other 1990s OPE values that were corrected for deposition losses, which, for example, yielded adjusted OPE values between  $3:1$  and  $5:1$  near Nashville in 1995 (Nunnermacker et al., 1998; St John et al., 1998; Sillman et al., 1998). Our higher observed OPE values after 2010 are consistent with aircraft measurements made in the



Southeast in August and September 2013, which show  $O_x (= O_3 + NO_2)$  versus  $NO_z$  slope of 17.4, and they are also consistent with model calculations, which show slopes of 14.1 to 16.7 (Travis et al., 2016). For comparability, we note that our  $O_3$  versus  $NO_z$  regression slopes were 13.1 to 18.8 ( $\pm 1.2$  to 1.4) in June and July, 2013, at three of four sites ( $25.7 \pm 2.8$  at the fourth site, which is the most rural in character) and our  $O_x$  versus  $NO_z$  slopes were 12.0 to 18.9 ( $\pm 1.2$  to 1.4) at three of the four sites ( $25.8 \pm 2.8$  at the fourth site). The increase in recently observed OPE that we report is therefore supported by the 2013 data of Travis et al. (2016). Our apparently high OPE values are also consistent with observation-based OPE that averaged 12.9 in ship plumes and 33.5 in assumed background marine air, as reported by Kim et al. (2016) using data from a 2002 study of ship emission plumes off the coast of southern California.

The increase in OPE with decreasing ambient  $NO_x$  and  $NO_z$  is also consistent with computations by Liu et al. (1987), which show relatively constant summer OPE of  $\sim 7 - 10$  for ambient  $NO_x$  exceeding  $\sim 7$  ppbv, increases in OPE to  $\sim 20$  as  $NO_x$  declines from  $\sim 7$  to  $\sim 1$  ppbv, more rapid increases in OPE to  $\sim 60$  as  $NO_x$  further declines to  $\sim 0.1$  ppbv, and a final slower increase of OPE to  $\sim 80$  as  $NO_x$  declines to  $\sim 0.01$  ppbv. While the numerical results of the modeling calculations by Liu et al. (1987) are specific to the modeled conditions, increasing OPE results from multiple factors that are pertinent to other conditions, such as radical reactions involving VOCs and  $NO_x$  (Lin et al., 1988).

In contrast to southern California, where Pollack et al. (2013) reported a shift from PAN to  $HNO_3$  production with no change in OPE, the SEARCH data exhibit an increase in observed OPE and do not definitively show a changing fraction of  $HNO_3$  relative to  $NO_y$ . Increasing formation of PAN (which regenerates  $NO_2$ ) and decreasing formation of  $HNO_3$  (which terminates cycling between  $NO$  and  $NO_2$ ) could increase OPE or otherwise facilitate  $O_3$  accumulation as ambient  $NO_x$  and  $NO_z$  mixing ratios continue to decline. Since the long-term SEARCH data record does not include measurements of PAN, this possible effect could not be investigated.

#### 4.4.3 Future $O_3$ Responses

Where  $NO_x$  limits reaction rates,  $O_3$  production is the product of OPE and ambient  $NO_x$  mixing ratios as determined for specific ambient conditions (Liu et al., 1987), so  $O_3$  reductions depend on changes in both OPE and  $NO_x$ . Increasing OPE offsets decreasing mixing ratios of  $NO_x$ , at least in part, so that  $O_3$  reductions are less than proportional to  $NO_x$  emission reductions. At present, there is no clear indication from the SEARCH data that OPE will continue to increase, begin decreasing, or level off. SEARCH data do not indicate that OPE has declined in recent years. The post-1990s  $O_3$  trend provides one guide to future average rates of  $O_3$  reduction in the sense that the rates of  $O_3$  reduction during the next decade are unlikely to deviate dramatically from those of the recent past. This result would be expected if OPE remains roughly constant or even decreases somewhat, as indicated in Figure 10 for the years since about 2009. If OPE were to increase faster than  $NO_x$  mixing ratios decreased,  $O_3$  maxima would tend to increase with declining  $NO_x$ . If OPE were to start declining as  $NO_x$  emissions and mixing ratios continue to decrease,  $O_3$  maxima would decline less dramatically in the next few years compared with the past 6 - 7 years. At the limit of OPE approaching zero,  $O_3$  maxima would level off and no further  $O_3$  reductions would occur. From the observations to date, this condition appears to be well below ambient  $NO_z$  levels of  $\sim 0.2$  ppbv. Previous work indicates that





VOC reactivity and O<sub>3</sub> losses contribute to nonlinearity; at ambient NO<sub>x</sub> mixing ratios less than ~0.4 ppbv, O<sub>3</sub> loss suppresses OPE, and below ~80 pptv NO<sub>x</sub>, OPE becomes negative (Lin et al., 1988).

The future O<sub>3</sub>-NO<sub>z</sub> relationships are contingent on continuing an unspecified historical response to VOC changes. Anthropogenic VOC mixing ratios have declined since 1999, but natural components such as isoprene and terpene mixing ratios have remained relatively constant (Figure 6; Blanchard et al., 2010a; Hidy et al., 2014). Evidence suggests that O<sub>3</sub> formation in the SEARCH region will move toward more NO<sub>x</sub> sensitive conditions with continued decreases in NO<sub>x</sub> emissions and more limited declines in anthropogenic VOC emissions, coupled with high levels of natural VOC emissions in the region. This anticipated emission reduction path should reinforce the O<sub>3</sub>-NO<sub>z</sub> relationships and the OPE interpretation presented here.

## 5 Conclusions

Summer O<sub>3</sub> mixing ratios declined along with decreasing emissions in the southeastern U.S. between 1999 and 2014. The seasonal variability of the highest peak daily 8-hour O<sub>3</sub> mixing ratios also declined over time: summer monthly O<sub>3</sub> maxima declined more than other monthly maxima, while winter monthly maxima of ~40 ppbv occurred throughout the period of record. Higher mean monthly 2 p.m. O<sub>3</sub> mixing ratios are associated with higher mean ratios of NO<sub>z</sub>/NO<sub>y</sub>, indicating that more O<sub>3</sub> formation and accumulation occurs when more NO<sub>x</sub> has been converted to reaction products by early afternoon, especially for mean NO<sub>z</sub>/NO<sub>y</sub> exceeding ~0.6. Higher mean mid-day O<sub>3</sub> mixing ratios and higher ratios of mean NO<sub>z</sub>/NO<sub>y</sub> occur in summer compared to other seasons.

The summer O<sub>3</sub> trend is less than 1:1 proportional to precursor changes, as indicated by observed relationships of O<sub>3</sub> to NO<sub>z</sub>, which is the product of reactions involving NO<sub>x</sub>. Observationally-determined OPE increases as ambient mixing ratios of NO<sub>x</sub> oxidation products decline, partially offsetting precursor decreases and contributing to the nonlinear O<sub>3</sub> response, but also suggesting increasing responsiveness of O<sub>3</sub> to NO<sub>x</sub>. The effectiveness of ongoing NO<sub>x</sub> emission reductions on peak O<sub>3</sub> values will depend on the balance between changes in observed OPE and ambient NO<sub>x</sub>, in the context of ongoing VOC changes. In addition, changes in the relative importance of chemical reactions that yield HNO<sub>3</sub> compared with PAN are likely to play a role in altering OPE and O<sub>3</sub> accumulation. The past O<sub>3</sub> response to NO<sub>x</sub> emission reductions exhibits seasonal variability, which will have potentially important implications for future O<sub>3</sub> management if spring and autumn O<sub>3</sub> maxima fail to decline and thereby become a focus of concern that merits attention comparable to summer O<sub>3</sub> maxima.

## Data Availability

The SEARCH data are available at <https://www.dropbox.com/sh/o9hxoa4wlo97zpe/AACbm6LetQowrpUgX4vUxnoDa?dl=0>. EPA data are available at [http://aqsdrl.epa.gov/aqswweb/aqstmp/airdata/download\\_files.html](http://aqsdrl.epa.gov/aqswweb/aqstmp/airdata/download_files.html) and at <https://www.epa.gov/castnet>.



## Author Contributions

C. L. B. and G. M. H. designed the study and wrote the manuscript. C. L. B. carried out the statistical analyses.

## Competing Interests

The authors declare that they have no conflict of interest.

## 5 Acknowledgments

The authors thank Atmospheric Research and Analysis, Inc. for collecting, validating, and providing SEARCH data, and J. Jansen for managing the SEARCH study. Funding for the SEARCH network was provided by Southern Company with contributions from the Electric Power Research Institute. Southern Company provided partial financial support for analysis of SEARCH data. We are indebted to these sponsors for supporting this unique long-term measurement program.

## 10 References

- Arif, N. L. and A. M. Abdullah: Ozone pollution and historical trends of surface background ozone level: a review, *World Applied Sciences Journal*, 14 (Exploring Pathways to Sustainable Living in Malaysia: Solving the Current Environmental Issues), 31-38, 2011.
- Atkinson, R.: Atmospheric chemistry of VOCs and NO<sub>x</sub>, *Atmos. Environ.*, 34, 2063 – 2101, 2000.
- 15 Atmospheric Research and Analysis (ARA): <https://www.dropbox.com/sh/o9hxo4wlo97zpe/AACbm6LetQowrpUgX4vUxnoDa?dl=0> (last access April 24, 2017), 2017.
- Blanchard, C.L., S. Tanenbaum, G. Hidy, R. Rasmussen, and R. Watkins: NMOC, ozone and organic aerosol in the southeastern states, 1999-2007. 1. Spatial and temporal variations of NMOC mixing ratios and composition in Atlanta, Georgia, *Atmos. Environ.*, 44, 4827-4839, 2010a.
- 20 Blanchard, C. L., G. M. Hidy, and S. Tanenbaum: NMOC, ozone, and organic aerosol in the southeastern states, 1999-2007: 2. Ozone trends and sensitivity to NMOC emissions in Atlanta, Georgia. *Atmos. Environ.* 44: 4840 – 4849. doi:10.1016/j.atmosenv.2010.07.030, 2010b.
- Blanchard, C. L., G. M. Hidy, S. Tanenbaum, E. S. Edgerton, and B. E. Hartsell: The Southeastern Aerosol Research and Characterization (SEARCH) study: Spatial variations and chemical climatology, 1999 – 2010, *J. Air Waste Manage. Assoc.*,
- 25 63, 260-275, doi:10.1080/10962247.2012.749816, 2014.
- Blanchard, C. L., S. Tanenbaum, and G. Hidy: Ozone in the southeastern United States: an observation-based model using measurements from the SEARCH network, *Atmos. Environ.*, 48, 192-200, 2014.



- Chameides, W. and E. Cowling: The State of the Southern Oxidants Study: Policy Relevant Findings in Ozone Pollution Research, 1988-1994, Southern Oxidant Study, College of Forest Resources, North Carolina State University, Raleigh, NC, 1995.
- Chan, E.: Regional ground-level ozone trends in the context of meteorological influences across Canada and the eastern United States from 1997 to 2006, *J. Geophys. Res. Atmos.*, 114, D05301, doi:10.1029/2008JD010090, 2009.
- Chan, E. and R. J. Vet, R. J.: Baseline levels and trends of ground level ozone in Canada and the United States, *Atmos. Chem. Phys.*, 10, 8629-8647, doi:10.5194/acp-10-8629-2010, 2010.
- Cooper, O., R-S. Gao, D. Tarasick, T. Leblanc, and C. Sweeney: Long-term ozone trends at rural ozone monitoring sites across the United States, 1990-2010, *J. Geophys. Res. Atmos.*, 117, D22307, 2012.
- Cooper, O., D. Parrish, J. Ziemke, N. Balashov, M. Cupeiro, I. Galbally, S. Gilge, I. Horowitz, N. Jensen, J. Larmarque, N. Naik, S. Oltmans, J. Schwab, D. Shindell, A. Thompson, V. Thouret, Y. Wang, and R. Zhinden: Global distribution and trends of tropospheric ozone: an observation-based review, *Elementa*, 2, 1-28, doi:10.12952/journalelementa.000029, 2014.
- Dolwick, P., F. Akhtar, K. R. Baker, N. Possiel, and H. Simon: Comparison of background ozone estimates over the western United States based on two separate model methodologies, *Atmos. Environ.*, 109, 282-296, <http://dx.doi.org/10.1016/j.atmosenv.2015.01.005>, 2015.
- Cristofanelli, P. and P. Bonasoni: Background ozone in the southern Europe and Mediterranean area: influence of the transport processes, *Environ. Pollut.*, 157 (5), 1399-1406, doi.org/10.1016/j.envpol.2008.09.017, 2009.
- Edgerton, E. S., R. D. Saylor, B. E. Hartsell, J. J. Jansen, and D. A. Hansen: Ammonia and ammonium measurements from the southeastern United States, *Atmos. Environ.*, 41(16), 3339-3351, 2007.
- Fiore, A., J. T. Oberman, M.Y. Lin, L. Zhang, O.E. Clifton, D. J. Jacob, V. Naik, L. W. Horowitz, J. P. Pinto, and G. Milly: Estimating North American background ozone in U.S. surface air with two independent global models: variability, uncertainties, and recommendations, *Atmos. Environ.*, 96, 284-300, 2014.
- Frost, G. J., M. Trainer, G. Allwine, M. P. Buhr, J. G. Calvert, C. A. Cantrell, F. C. Fehsenfeld, P. D. Goldan, J. Herwehe, G. Hubler, W. C. Kuster, R. Martin, R. T. McMillen, S. A. Montzka, R. B. Norton, D. D. Parrish, B. A. Ridley, R. E. Shetter, J. G. Walega, B. A. Watkins, H. H. Westberg, and E. J. Williams: Photochemical ozone production in the rural southeastern United States during the 1990 Rural Oxidants in the Southern Environment (ROSE) program, *J. Geophys. Res. Atmos.*, 103(D17), 22491-22508, 1998.
- Fujita, E., W. Stockwell, D. Campbell, R. Keisslar, and D. Lawson: Evolution of the magnitude and spatial extent of the weekend ozone effect in California's South Coast Air Basin, 1981-2000, *J. Air Waste Manage. Assoc.*, 53, 802-815, 2003.
- Fujita, E., D. E. Campbell, W. Stockwell, E. Saunders, R. Fitzgerald, and R. Perea: Projected ozone trends and changes in the ozone-precursor relationship in the South Coast Air Basin in response to varying reductions of precursor emissions, *J. Air Waste Manage. Assoc.*, 66(2), 201 – 214, 2015.



- Godowitch, J.M., R. C. Gilliam, and S. T. Rao: Diagnostic evaluation of ozone production and horizontal transport in a regional photochemical air quality modeling system, *Atmos. Environ.*, 45 (24) 3977-3987, 2011.
- de Gouw, J. A., D. D. Parrish, G. J. Frost, and M. Trainer: Reduced emissions of CO<sub>2</sub>, NO<sub>x</sub>, and SO<sub>2</sub> from U.S. power plants owing to switch from coal to natural gas with combined cycle technology, *Earth's Future*, 2, 75-82, doi: 10.1002/2013EF000196, 2014.
- 5 Griffin, R. J., C. A. Johnson, R. W. Talbot, H. Mao, R. S. Russo, Y. Zhou, and B. C. Sive: Quantification of ozone formation metrics at Thompson Farm during the New England Air Quality Study (NEAQS) 2002, *J. Geophys. Res. Atmos.*, 109(D24), D24302, doi:10.1029/2004JD005344, 2004.
- Hansen, D.A., E. S. Edgerton, B. E. Hartsell, J. J. Jansen, G. M. Hidy, K. Kandasamy, and C. L. Blanchard: The Southeastern Aerosol Research and Characterization Study (SEARCH): 1. Overview, *J. Air Waste Manage. Assoc.*, 53, 1460-1471, 2003.
- 10 Hansen, D. A., E. Edgerton, B. Hartsell, J. Jansen, H. Burge, P. Koutrakis, C. Rogers, H. Suh, J. Chow, B. Zielinska, P. McMurry, J. Mulholland, A. Russell, and R. Rasmussen: Air quality measurements for the aerosol research and inhalation epidemiology study, *J. Air Waste Manage. Assoc.*, 56, 1445-1458, 2006.
- He, H., L. Hembeck, K. M. Hosley, T. P. Canty, R. J. Salawitch, and R. R. Dickerson: High ozone concentrations on hot days: The role of electric power demand and NO<sub>x</sub> emissions, *Geophys. Res. Lett.*, 40, 5291-5294, doi:10.1002/grl.50967, 2013.
- 15 Hidy, G. M. and C. L. Blanchard: Precursor reductions and ground-level ozone in the continental U.S., *J. Air Waste Manage. Assoc.*, 65(10), 1261 – 1282, doi: 10.1080/10962247.2015.1079564. <http://dx.doi.org/10.1080/10962247.2015.1079564> (last access August 2, 2017), 2015.
- Hidy, G., C. Blanchard, K. Baumann, E. Edgerton, S. Tanenbaum, S. Shaw, E. Knipping, I. Tombach, J. Jansen and J. Walters: Chemical climatology of the southeastern United States, 1999-2013, *Atmos. Chem. Phys.*, 14, 11893-11914, 2014.
- 20 Hirsch, A. I., J. W. Munger, D. J. Jacob, L. W. Horowitz, and A. H. Goldstein: Seasonal variation of the ozone production efficiency per unit NO<sub>x</sub> at Harvard Forest, Massachusetts, *J. Geophys. Res. Atmos.*, 101(D7), 12659-12666, doi:10.1029/96JD00557, 1996.
- Hudman, R.C., D. J. Jacob, S. Turquety, E. M. Leibensperger, L. T. Murray, S. Wu, A. B. Gilliland, M. Avery, T. H. Bertram, W. Brune, R. C. Cohen, J. E. Dibb, F. M. Flocke, A. Fried, J. Holloway, J. A. Neuman, R. Orville, A. Perring, X. Ren, G. W.
- 25 Sachse, H. B. Singh, A. Swanson, and P. J. Wooldridge: Surface and lightning sources of nitrogen oxides over the United States: Magnitudes, chemical evolution, and outflow, *J. Geophys. Res. Atmos.*, 112, D12S05, doi:10.1029/2006JD007912, 1997.
- Jacob, D. J., L. W. Horowitz, J. W. Munger, B. G. Heikes, R. R. Dickerson, R. S. Artz, and W. C. Keene: Seasonal transition from NO<sub>x</sub>- to hydrocarbon-limited conditions for ozone production over the Eastern United States in September, *J. Geophys. Res. Atmos.*, 100 (D5), 9315- 9324, 1995.
- 30 Kasibhatla, P., W. L. Chameides, R. D. Saylor, and D. Olerud: Relationships between regional ozone pollution and emissions of nitrogen oxides in the eastern United States, *J. Geophys. Res. Atmos.*, 103(D17), 22663-22669, doi:10.1029/98JD01639, 1998.



- Kim, H. S., Y. H. Kim, K. M. Han, J. Kim, and C. H. Song: Ozone production efficiency of a ship-plume: ITCT 2K2 case study, *Chemosphere*, 143, 17-23, 2016.
- Kleinman, L.I., P.H Daum, Y.N Lee, G.I. Senum, S.R. Springston, J. Wany, C. Berkowitz, J. Hubbe, R.A. Zaveri, F.J. Brechtel, J. Jayne, T.B. Onasch, and D. Worsnop: Aircraft observations of aerosol composition and ageing in New England and mid-Atlantic states during the summer 2002 New England Air Quality Study field campaign. *J. Geophys. Res. Atmos.*, 112, D09310. doi:10.1029/2006JD007786, 2007.
- 5 Kleinman, L., Y.-N. Lee, S. R. Springston, L. Nunnermacker, X. Zhou, R. Brown, K. Hallock, P. Klotz, D. Leahy, J. H. Lee, and L. Newman: Ozone formation at a rural site in the southeastern United States, *J. Geophys. Res. Atmos.*, 99(D2), 3469-3482, doi:10.1029/93JD02991, 1994.
- 10 Langford, A.O., C.J. Senff, R.J. Alvarez II, J. Brioude, O.R. Cooper, J.S. Holloway, M.Y. Lin, R.D. Marchbanks, R.B. Pierce, S.P. Sandberg, A.M. Weickmann, and E.J. Williams: An overview of the 2013 Las Vegas Ozone Study (LVOS): Impact of stratospheric intrusions and long-range transport on surface air quality, *Atmos. Environ.* 109 (2015) 305-322, 2015.
- Lefohn, A., D. Shadwick, and S. Oltmans: Characterizing changes in surface ozone levels in metropolitan and rural areas in the United States for 1980-2008 and 1994-2008, *Atmos. Environ.*, 44, 5199-5210, 2010.
- 15 Lefohn, A., C. Emery, D. Shadwick, H. Wernli, J. Jung, and S. Oltmans: Estimates of background surface ozone mixing ratios in the United States based on model-derived source apportionment, *Atmos. Environ.*, 84, 275-288, doi:10.1016/j.atmosenv.2013.11.033, 2014.
- Lin, X., M. Trainer, and S. C. Liu: On the nonlinearity of the tropospheric ozone production., *J. Geophys. Res. Atmos.*, 93(D12), 15879 – 15888, 1988.
- 20 Lin, M., A. M. Fiore, O. R. Cooper, L. W. Horowitz, A. O. Langford, H. Levy, B. J. Johnson, V. Naik, S. J. Oltmans, and C. J. Senff: Springtime high surface ozone events over the western United States: Quantifying the role of stratospheric intrusions, *J. Geophys. Res. Atmos.*, 117, D00V22, 2012.
- Liu, S. C., M. Trainer, F. C. Fehsenfeld, D. D. Parrish, E. J. Williams, D. W. Fahey, G. Hubler, and P. C. Murphy: Ozone production in the rural troposphere and the implications for regional and global ozone distributions, *J. Geophys. Res.*, 92(D4), 25 4191-4207, 1987.
- Logan, J.: Tropospheric ozone: seasonal behavior, trends, and anthropogenic influence., *J. Geophys. Res.*, 90(D6), 10463 – 10482, 1985.
- Meagher, J., E. Cowling, F. Fehsenfeld, and W. Parkhurst: Ozone formation and transport in southeastern United States: overview of the SOS Nashville/Middle Tennessee Study, *J. Geophys. Res.*, 103, 22,213-22,223, 1998.
- 30 McDuffie, E. E., P. M. Edwards, J. B. Gilman, B. M. Lerner, W. P. Dubé, M. Trainer, D. E. Wolfe, W. M. Angevine, J. deGouw, E. J. Williams, A. G. Tevlin, J. G. Murphy, E. V. Fischer, S. McKeen, T. B. Ryerson, J. Peischl, J. S. Holloway, K. Aikin, A. O. Langford, C. J. Senff, R. J. Alvarez II, S. R. Hall, K. O. Lantz and S. S. Brown: Influence of oil and gas emissions on summertime ozone in the Colorado Northern Front Range, *J. Geophys. Res. Atmos.*, 121, 8712-8729, doi:10.1002/2016JD025265, 2016.



- National Research Council: Rethinking the Ozone Problem in Urban and Regional Air Pollution, National Academy Press, Washington, D.C., 489 pp., 1991.
- NARSTO: An Assessment of Tropospheric Ozone Pollution, Report 1000040, NARSTO, Pasco, WA (also available from EPRI, Palo Alto, CA), 2000.
- 5 Naja, M., H. Akimoto, and J. Staehelin: Ozone in background and photochemically aged air over central Europe: Analysis of long-term ozonesonde data from Hohenpeissenberg and Payerne, *J. Geophys. Res.*, 108(D2), 4063, doi:10.1029/2002JD002477, 2003
- Neuman, J. A., J. B. Nowak, W. Zheng, F. Flocke, T. B. Ryerson, M. Trainer, J. S. Holloway, D. D. Parrish, G. J. Frost, J. Peischl, E. L. Atlas, R. Bahreini, A. G. Wollny, and F. C. Fehsenfeld: Relationship between photochemical ozone production and NO<sub>x</sub> oxidation in Houston, Texas, *J. Geophys. Res. Atmos.*, 114, D00F08, doi:10.1029/2008JD011688, 2009.
- 10 Neuman, J. A., M. Trainer, S. S. Brown, K.-E. Min, J. B. Nowak, D. D. Parrish, J. Peischl, I. B. Pollack, J. M. Roberts, T. B. Ryerson, and P. R. Veres: HONO emission and production determined from airborne measurements over the Southeast U.S., *J. Geophys. Res. Atmos.*, 121, 9237–9250, doi:10.1002/2016JD025197, 2016.
- Nunnermacker, L. J., D. Imre, P. H. Daum, L. Kleinman, Y.-N. Lee, J. H. Lee, S. R. Springston, L. Newman, J. Weinstein-  
15 Lloyd, W. T. Luke, R. Banta, R. Alvarez, C. Senff, S. Sillman, M. Holdren, G. W. Keigley, and X. Zhou: Characterization of the Nashville urban plume on July 3 and July 18, 1995, *J. Geophys. Res. Atmos.*, 103(D21), 28129-28148, doi:10.1029/98JD01961, 1998.
- Oltmans, S., A. Lefohn, J. Harris, and D. Shadwick: Background ozone levels of air entering the west coast of the US and assessment of longer-term changes, *Atmos. Environ.*, 42, 6020-6038, 2008.
- 20 Oltmans, S., A. Lefohn, D. Shadwick, J. Harris, H. Scheel, I. Galbally, D. Tarasick, B. Johnson, E. Brunke, H. Claude, G. Zeng, S. Nichol, F. Schmidlin, J. Davies, E. Cuevas, A. Redondas, H. Naoe, T. Kakano, and T. Kawasato: Recent tropospheric ozone changes – a pattern dominated by slow or no growth, *Atmos. Environ.*, 67, 331-351, 2013.
- Ordóñez, C., D. Brunner, J. Staehelin, P. Hadjinicolaou, J. A. Pyle, M. Jonas, H. Wernli, and A. S. H. Prévôt: Strong influence of lowermost stratospheric ozone on lower tropospheric background ozone changes over Europe, *Geophys. Res. Lett.*, 34, L07805,  
25 doi:10.1029/2006GL029113, 2007.
- Paoletti, E., A. De Marco, D. C. S. Beddows, R. M. Harrison, and W. J. Manning: Ozone levels in European and USA cities are increasing more than at rural sites, while peak values are decreasing, *Environmental Pollution*, 192, 295-299, 2014.
- Pollack, I., T. Ryerson, M. Trainer, J. Neuman, J. Roberts, and D. Parrish: Trends in ozone its precursors and related secondary oxidation products in Los Angeles, California: a synthesis of measurements from 1960-2010, *J. Geophys. Res. Atmos.*, 118,  
30 5891-5911, 2013.
- Reynolds, S., C. L. Blanchard, and S. Ziman: Understanding the effectiveness of precursor reductions in lowering 8-hour ozone mixing ratios, *J. Air & Waste Manage. Assoc.*, 53, 195-205, 2003.
- Reynolds, S., C. L. Blanchard, and S. Ziman: Understanding the effectiveness of precursor reductions in lowering the 8-hr. O<sub>3</sub> concentration: part II-eastern United States, *J. Air & Waste Manage. Assoc.*, 54, 1452-1470, 2004.





- Ryerson, T. B., A. E. Andrews, W. M. Angevine, T. S. Bates, C. A. Brock, B. Cairns, R. C. Cohen, O. R. Cooper, J. A. de Gouw, F. C. Fehsenfeld, R. A. Ferrare, M. L. Fischer, R. C. Flagan, A. H. Goldstein, J. W. Hair, R. M. Hardesty, C. A. Hostetler, J. L. Jimenez, A. O. Langford, E. McCauley, S. A. McKeen, L. T. Molina, A. Nenes, S. J. Oltmans, D. D. Parrish, J. R. Pederson, R. B. Pierce, K. Prather, P. K. Quinn, J. H. Seinfeld, C. J. Senff, A. Sorooshian, J. Stutz, J. D. Surratt, M. Trainer, R. Volkamer, E. J. Williams, and S. C. Wofsy: The 2010 California Research at the Nexus of Air Quality and Climate Change (CalNex) field study, *J. Geophys. Res. Atmos.*, 118, 5830–5866, doi:10.1002/jgrd.50331, 2013.
- Saylor, R. D., E. S. Edgerton, B. E. Hartsell, K. Baumann, and D. A. Hansen: Continuous gaseous and total ammonia measurements from the southeastern aerosol research and characterization (SEARCH) study, *Atmos. Environ.*, 44, 4994–5004, 2010.
- Schere, K. and G. M. Hidy: Foreword: NARSTO critical reviews., *Atmos. Environ.*, 34, 1853 – 1860, 2000.
- Schnell, R. C., S. J. Oltmans, R. R. Neely, M. S. Endres, J. V. Molenaar, and A. B. White: Rapid photochemical production of ozone at high concentrations in a rural site during winter, *Nature Geoscience*, 2 (2), 120–122, doi:10.1038/ngeo415, 2009.
- Seigneur, C. and R. Dennis: Atmospheric modeling, in Hidy, G. M., J. R. Brook, K. L. Demerjian, Luisa T. Molina, W.T. Pennell, and R. D. Scheffe, eds., *Technical Challenges of Multipollutant Air Quality Management*, Springer, New York, 2011.
- Seinfeld, J. H.: *Atmospheric Chemistry and Physics of Air Pollution*, John Wiley and Sons, New York, 1986.
- Sillman, S., D. He, M. Pippin, P. H. Daum, D. G. Imre, L. I. Kleinman, and J. H. Lee: Model correlations for ozone, reactive nitrogen, and peroxides for Nashville in comparison with measurements: Implications for O<sub>3</sub>-NO<sub>x</sub>-hydrocarbon chemistry, *J. Geophys. Res. Atmos.*, 103(D17), 22629–22644, 1998.
- Simon, H., A. Reff, B. Wells, J. Xing, and N. Frank: Ozone trends across the United States over a period of decreasing NO<sub>x</sub> and VOC emissions, *Environ. Sci. Technol.*, 49(1), 186–195, <http://pubs.acs.org/doi/pdf/10.1021/es504514z>, 2015.
- Singh, H. B. and P. L. Hanst: Peroxyacetyl nitrate (PAN) in the unpolluted atmosphere: an important reservoir for nitrogen oxides, *Geophys. Res. Lett.*, 8, 941 – 944, 1981.
- Singh, H.: Reactive nitrogen in the troposphere: chemistry and transport of NO<sub>x</sub> and PAN, *Environ. Sci. & Technol.*, 21, 320 – 327, 1987.
- Solberg, S., R. G. Derwent, Ø. Hov, J. Langner, and A. Lindskog: European abatement of surface ozone in a global perspective, *Ambio*, 34(1): 47 – 53, [doi.org/10.1579/0044-7447-34.1.47](https://doi.org/10.1579/0044-7447-34.1.47), 2005.
- Solomon, P., Cowling, E., Hidy, G. and C. Furness: Comparison of scientific findings from major ozone field studies in North America and Europe. *Atmos. Environ.* 34. 1885–1920, 2000.
- St. John, J. C., W. L. Chameides, and R. Saylor: Role of anthropogenic NO<sub>x</sub> and VOC as ozone precursors: A case study from the SOS Nashville/Middle Tennessee Ozone Study, *J. Geophys. Res. Atmos.*, 103(D17), 22415–22423, 1998.
- Trainer, M., D. D. Parrish, M. P., Buhr, R. Norton, F. Fehsenfeld, K. Anlauf, J. Bottenheim, Y. Tang, H. Weibe, J. Roberts, R. Tanner, L. Newman, V. Bowersox, J. Meagher, K. Olszyna, M. Rodgers, T. Wang, H. Berresheim, K. Demerjian, and U. Roychowdhury: Correlation of ozone with NO<sub>y</sub> in photochemically aged air, *J. Geophys. Res. Atmos.*, 98(D2), 2917 – 2925, 1993.



- Trainer, M., B. A. Ridley, M. P. Buhr, G. Kok, J. Walega, G. Hübler, D. D. Parrish, and F. C. Fehsenfeld: Regional ozone and urban plumes in the southeastern United States: Birmingham, A case study, *J. Geophys. Res. Atmos.*, 100(D9), 18823- 18834, doi:10.1029/95JD01641, 1995.
- Trainer, M., D. Parrish, P. Goldan, P., J. Roberts, and F. Fehsenfeld: Review of observation-based analysis of regional factors influencing ozone concentration, *Atmos. Environ.*, 34, 2045-2062, 2000.
- Travis, K. R., D. J. Jacob, J. A. Fisher, P. S. Kim, E. A. Marais, L. Zhu, K. Yu, C. C. Miller, R. M. Yantosca, M. P. Sulprizio, A. M. Thompson, P. O. Wennberg, J. D. Crouse, J. M. St. Clair, R. C. Cohen, J. L. Laughner, J. E. Dibb, S. R. Hall, K. Ullmann, G. M. Wolfe, I. B. Pollack, J. Peischl, J. A. Neuman, and X. Zhou: Why do models overestimate surface ozone in the Southeast United States?, *Atmos. Chem. Phys.*, doi:10.5194/acp-16-13561-2016, 2016.
- U. S. EPA: Regional and Seasonal Analysis of North American Background Ozone Estimated from Two Studies, [http://www.epa.gov/ttn.naaqs/standards/ozone/data/20120814\\_Background\\_Ozone.pdf](http://www.epa.gov/ttn.naaqs/standards/ozone/data/20120814_Background_Ozone.pdf) (accessed January 2015), 2012.
- U.S. EPA: Health Risk and Exposure Assessment for Ozone Final Report, EPA-452/R-14-004a, <http://www.epa.gov/ttn/naaqs/standards/ozone/data/20140829healthrea.pdf>, (last access August 19, 2015), 2014.
- U.S. EPA: Ozone (O<sub>3</sub>) Standards - Documents from Current Review - Risk and Exposure Assessments, [http://www.epa.gov/ttn/naaqs/standards/ozone/s\\_o3\\_2008\\_rea.html](http://www.epa.gov/ttn/naaqs/standards/ozone/s_o3_2008_rea.html) (last access August 19, 2015), 2015a.
- U.S. EPA: Ozone (O<sub>3</sub>) Standards - Table of Historical Ozone NAAQS, [http://www.epa.gov/ttn/naaqs/standards/ozone/s\\_o3\\_history.html](http://www.epa.gov/ttn/naaqs/standards/ozone/s_o3_history.html) (last access August 19, 2015), 2015b.
- U.S. EPA: Environmental Protection Agency 40 CFR Parts 50, 51, 52, 53 and 58 [EPA-HQ-OAR-2008-0699; FRL-9918-43-OAR] RIN 2060-AP38, National Ambient Air Quality Standards for Ozone, <http://www.epa.gov/airquality/ozonepollution/pdfs/20141125proposal.pdf> (last access August 19, 2015), 2015c.
- U.S. EPA: National Trends in Ozone Levels, <http://www.epa.gov/airtrends/ozone.html> (last access August 19, 2015), 2015d.
- U.S. EPA: Air Quality Trends, <http://www.epa.gov/airtrends/aqtrends.html#comparison> (last access August 19, 2015), 2015e.
- U.S. EPA: AirData: Download Data Files. [http://aqsdr1.epa.gov/aqsweb/aqstmp/airdata/download\\_files.html](http://aqsdr1.epa.gov/aqsweb/aqstmp/airdata/download_files.html) (last access March 15, 2017), 2016a.
- U.S. EPA: Clean Air Status and Trends Network (CASTNET). <https://www.epa.gov/castnet> (last access March 24, 2016), 2016b.
- U.S. EPA: Air Markets Program Data. <http://ampd.epa.gov/ampd/> (last access September 12, 2016), 2016c.
- U.S. EPA: Air Pollutant Emission Trends Data. <https://www.epa.gov/air-emissions-inventories/air-pollutant-emissions-trends-data> (last access September 25, 2016), 2016d.
- Warneke, C., M. Trainer, J. A. de Gouw, et al.: Instrumentation and measurement strategy for the NOAA SENEX aircraft campaign as part of the Southeast Atmosphere Study 2013, *Atmos. Meas. Tech.*, 9, 3063-3093, doi:10.5194/amt-2015-388, 2016.



- Wilson, R. C., Z. L. Fleming, P. S. Monks, G. Clain, S. Henne, I. B. Konovalov, S. Szopa, and L. Menut: Have primary emission reduction measures reduced ozone across Europe? An analysis of European rural background ozone trends 1996–2005, *Atmos. Chem. Phys.*, 12, 437–454, doi:10.5194/acp-12-437-2012, 2012.
- Zaveri, R. A., C. M. Berkowitz, L. I. Kleinman, S. R. Springston, P. V. Doskey, W. A. Lonneman, and C. W. Spicer: Ozone production efficiency and NO<sub>x</sub> depletion in an urban plume: Interpretation of field observations and implications for evaluating O<sub>3</sub>-NO<sub>x</sub>-VOC sensitivity, *J. Geophys. Res. Atmos.*, 108 (D14), doi:10.1029/2002JD003144, 2003.
- Zhang, L., D. J. Jacob, N. V. Downey, D. A. Wood, D. Blewitt, C. C. Carouge, A. van Donkelaar, D. B. A. Jones, L. T. Murray, and Y. Wang: Improved estimate of the policy-relevant background ozone in the United States using the GEOS-Chem global model with  $1/2^\circ \times 2/3^\circ$  horizontal resolution over North America, *Atmos. Environ.*, 45 (37), 6769 – 6776, doi.org/10.1016/j.atmosenv.2011.07.054, 2011.

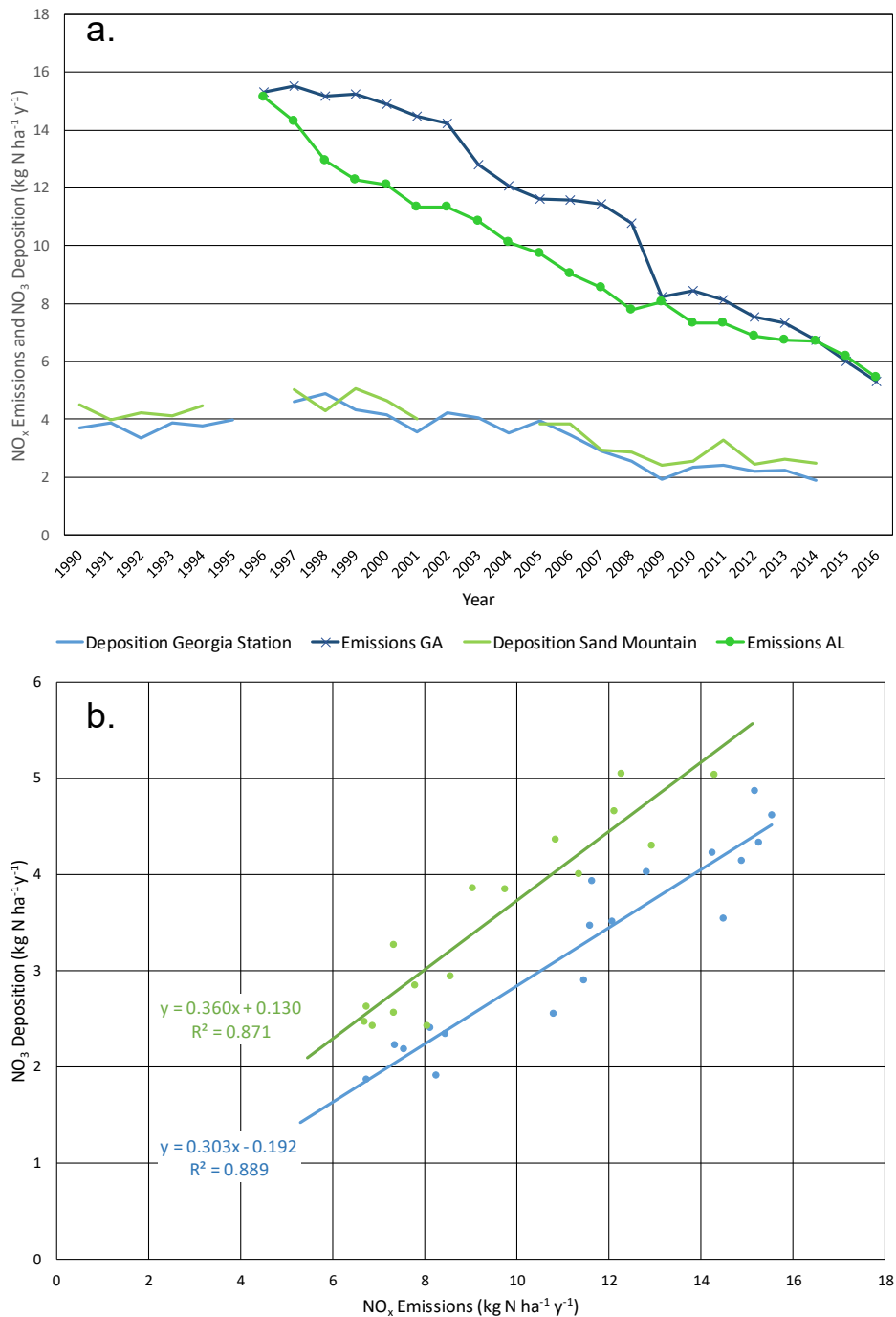
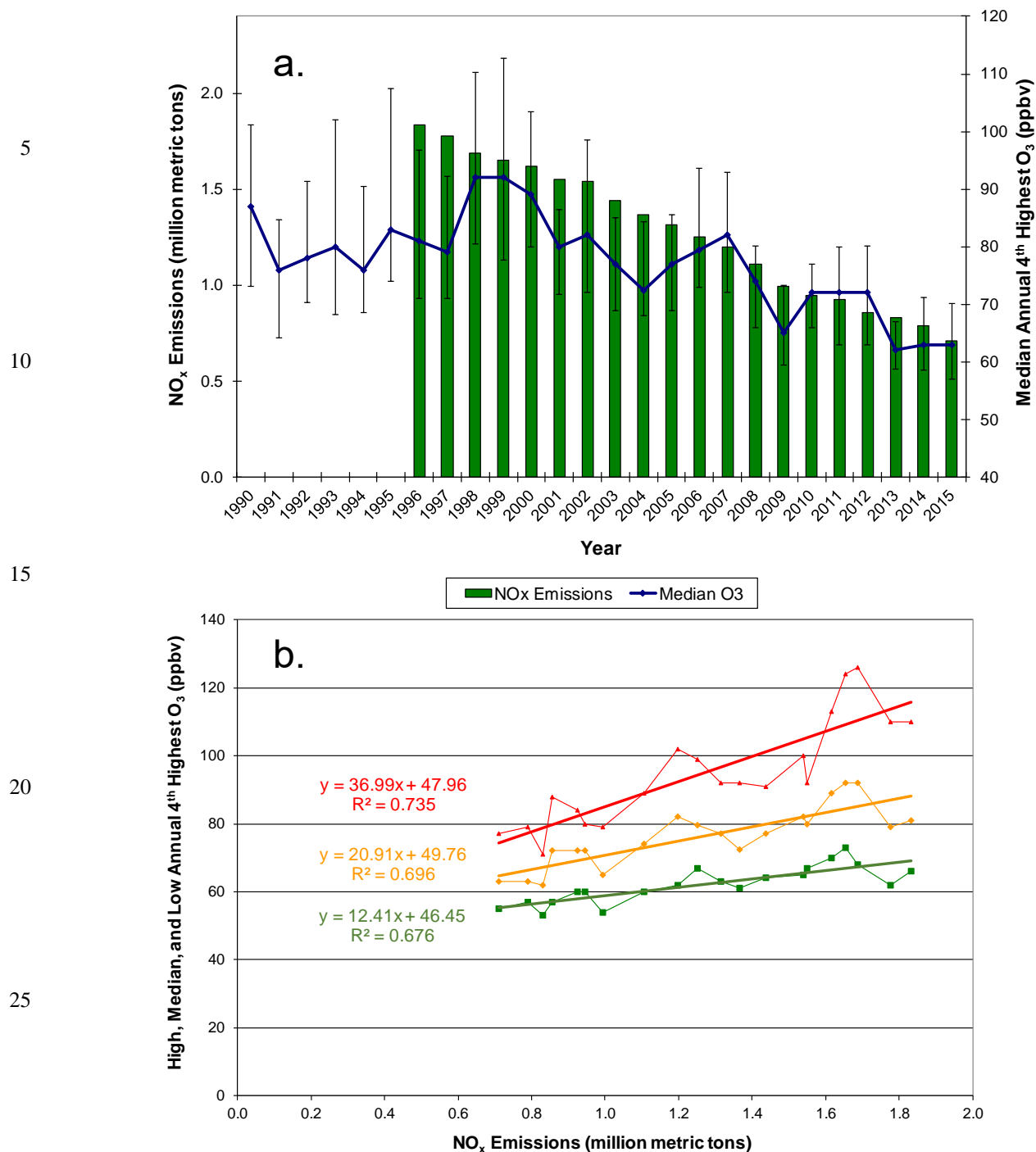


**Figure 1.** Comparison of nitrate deposition (wet plus dry) to NO<sub>x</sub> emission densities in Georgia and Alabama (a) trends and (b) regression (with same color coding in both panels). Nitrate deposition and NO<sub>x</sub> emission densities are expressed as kg ha<sup>-1</sup> y<sup>-1</sup>. NO<sub>x</sub> emissions are from all source sectors (supplement). Slopes are statistically significant ( $p < 0.0001$ ) and intercepts are not ( $p > 0.1$ ).



30 **Figure 2.** Comparison of annual 4<sup>th</sup>-highest daily peak 8-hour O<sub>3</sub> to NO<sub>x</sub> emissions in Georgia and Alabama (a) trends (+90<sup>th</sup> percentile site, -10<sup>th</sup> percentile site) and (b) regression. NO<sub>x</sub> emissions are from all source sectors (supplement). O<sub>3</sub> data include all EPA AQS monitors in Georgia and Alabama for each year having at least 75% data completeness (mean = 55 monitors, low of 32 – 36 in 1990 – 1993). Slopes and intercepts are statistically significant ( $p < 0.0001$ ).

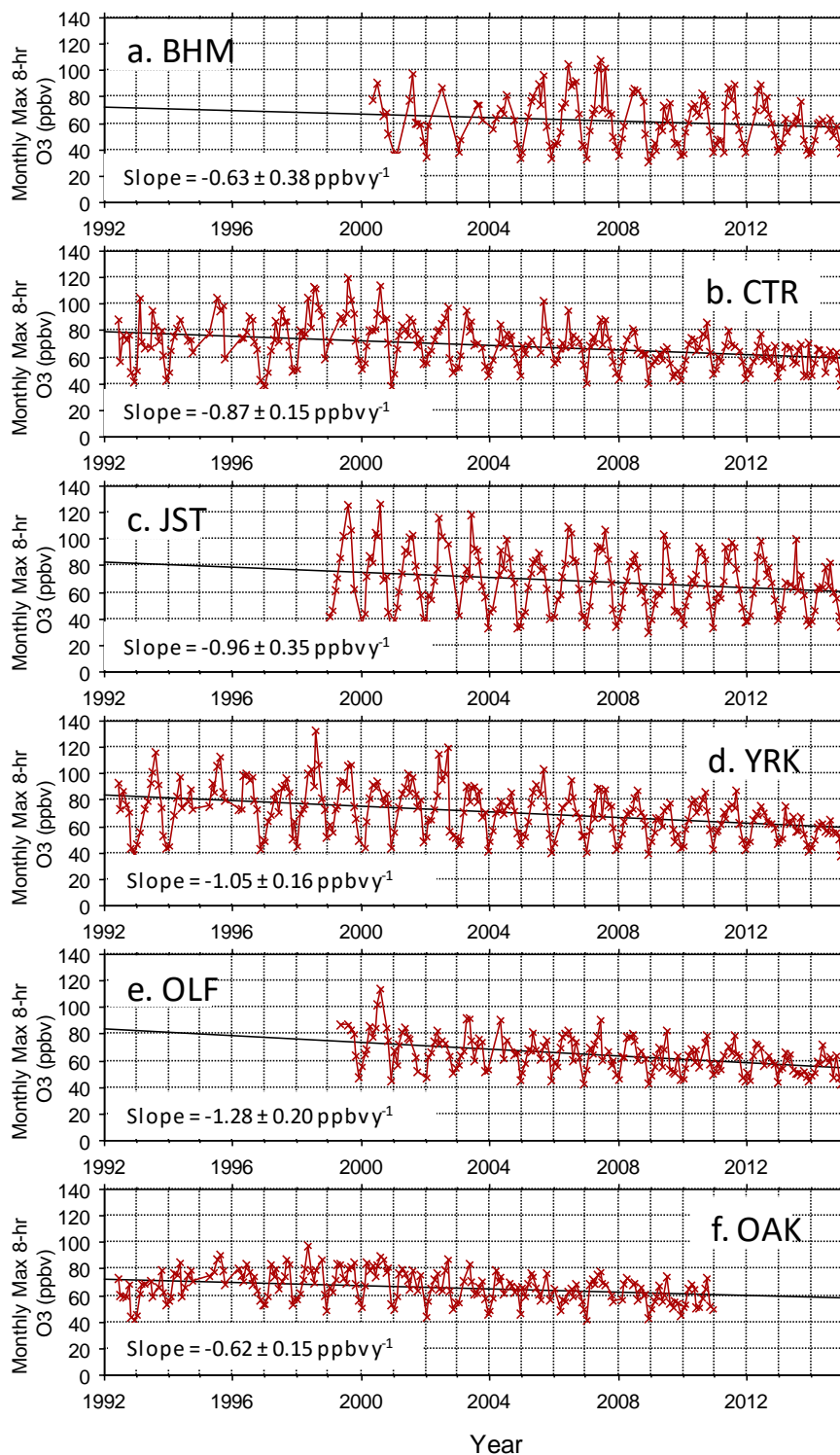
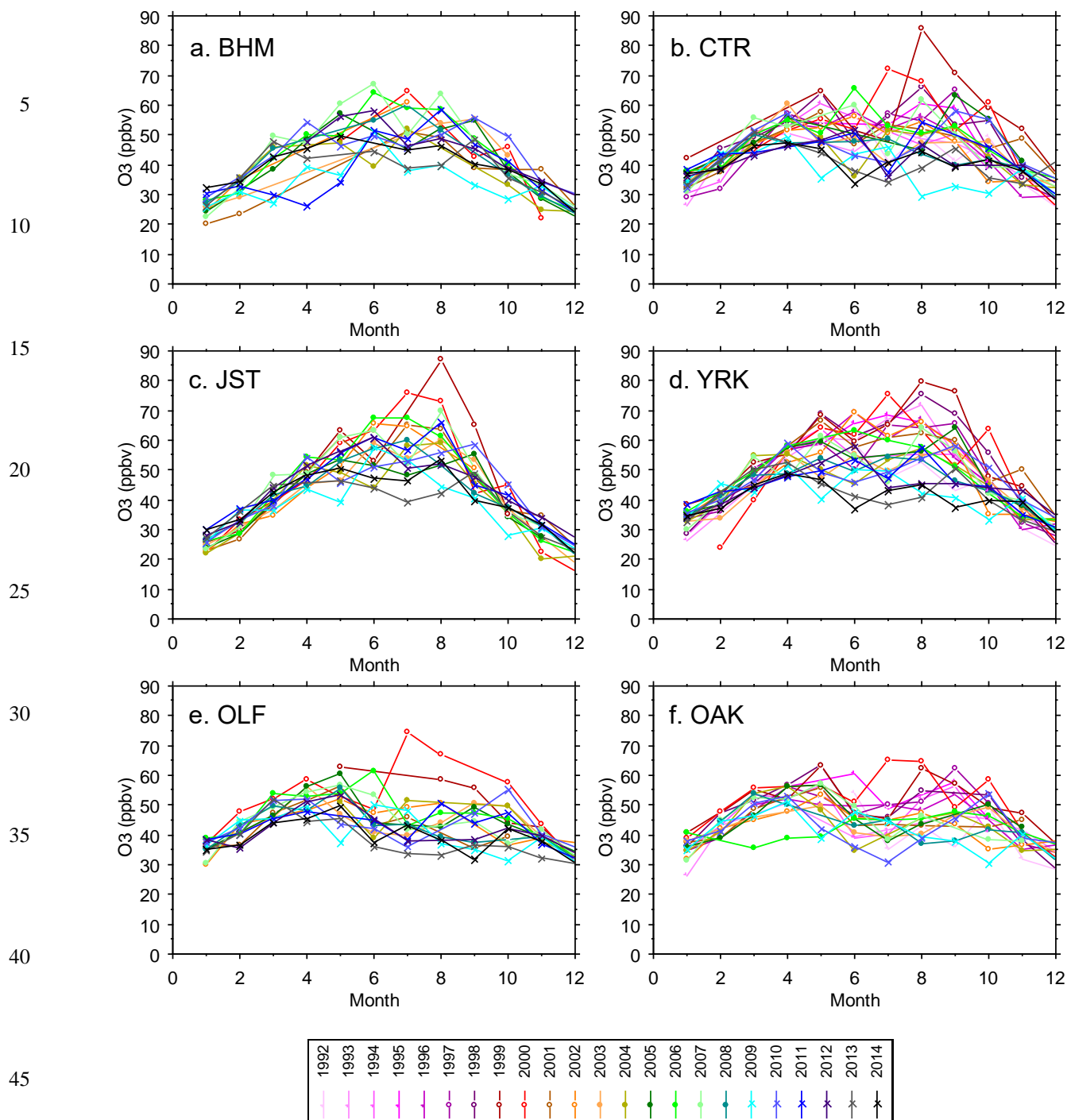


Figure 3. Monthly maxima of daily peak 8-hour average O<sub>3</sub> mixing ratios. All monthly maxima are determined from 24 or more days with 18 or more sampling hours per day. PNS and GFP (not shown) exhibit trends of  $-1.64 \pm 0.45$  and  $-0.60 \pm 0.32$  ppbv y<sup>-1</sup>, respectively. Trends are statistically significant ( $p < 0.01$ ) at CTR, JST, OAK, OLF, PNS, and YRK.





**Figure 4.** Monthly means of daily peak 8-hour average O<sub>3</sub> mixing ratios. All monthly means are determined from 24 or more days with 18 or more sampling hours per day.

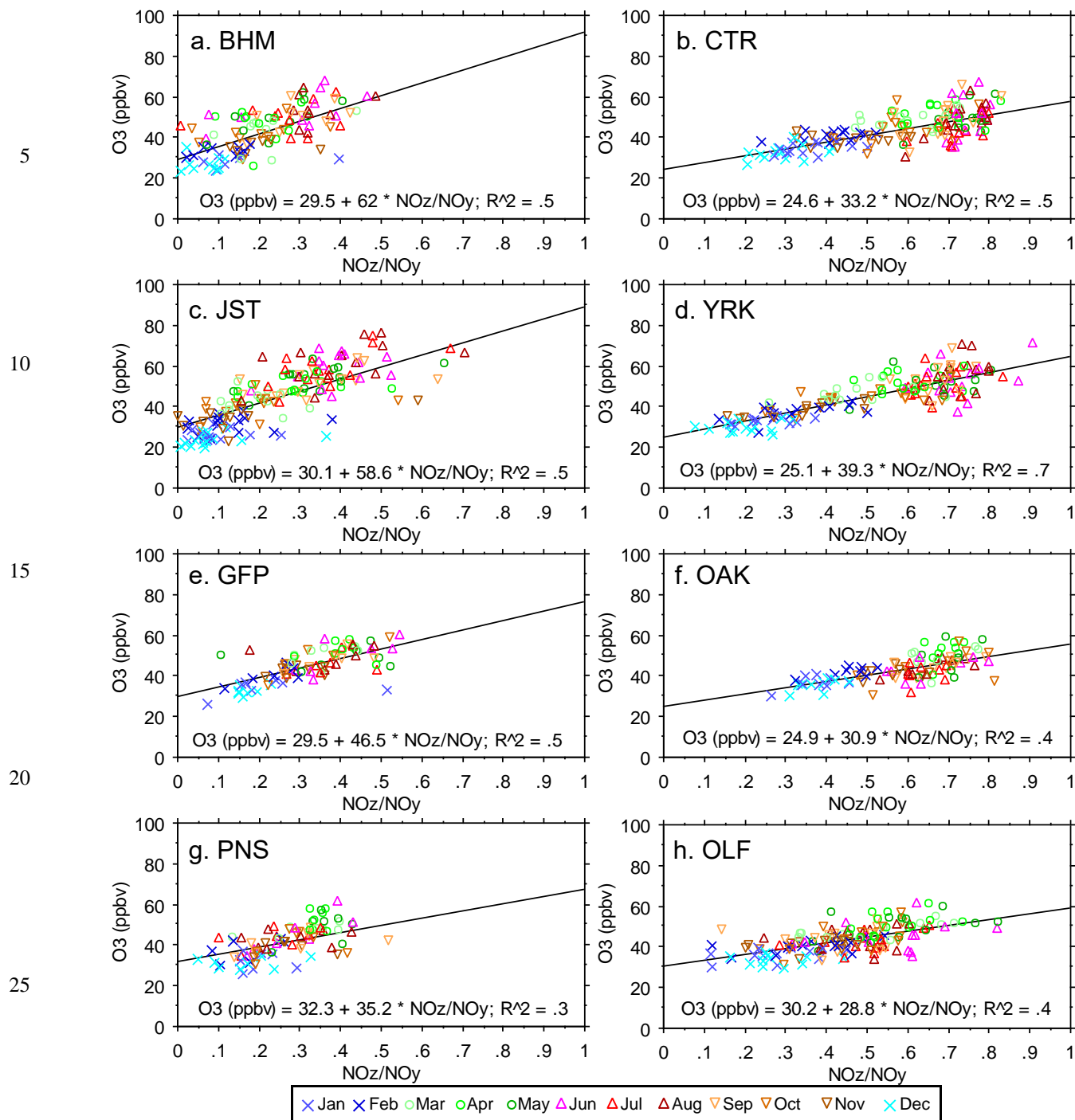


Figure 5. Mean monthly 2 p.m.  $O_3$  vs. mean monthly 2 p.m.  $NO_z/NO_y$ , 1999 – 2014. Each symbol is the monthly mean for one year. Standard errors of the monthly means average 2.5 ppbv  $O_3$  and 0.075 (dimensionless)  $NO_z/NO_y$ . Linear regression yields site-dependent slopes of 31 - 62 ppbv  $O_3$  per unit  $NO_z/NO_y$  (statistically significant,  $p < 0.0001$ ).

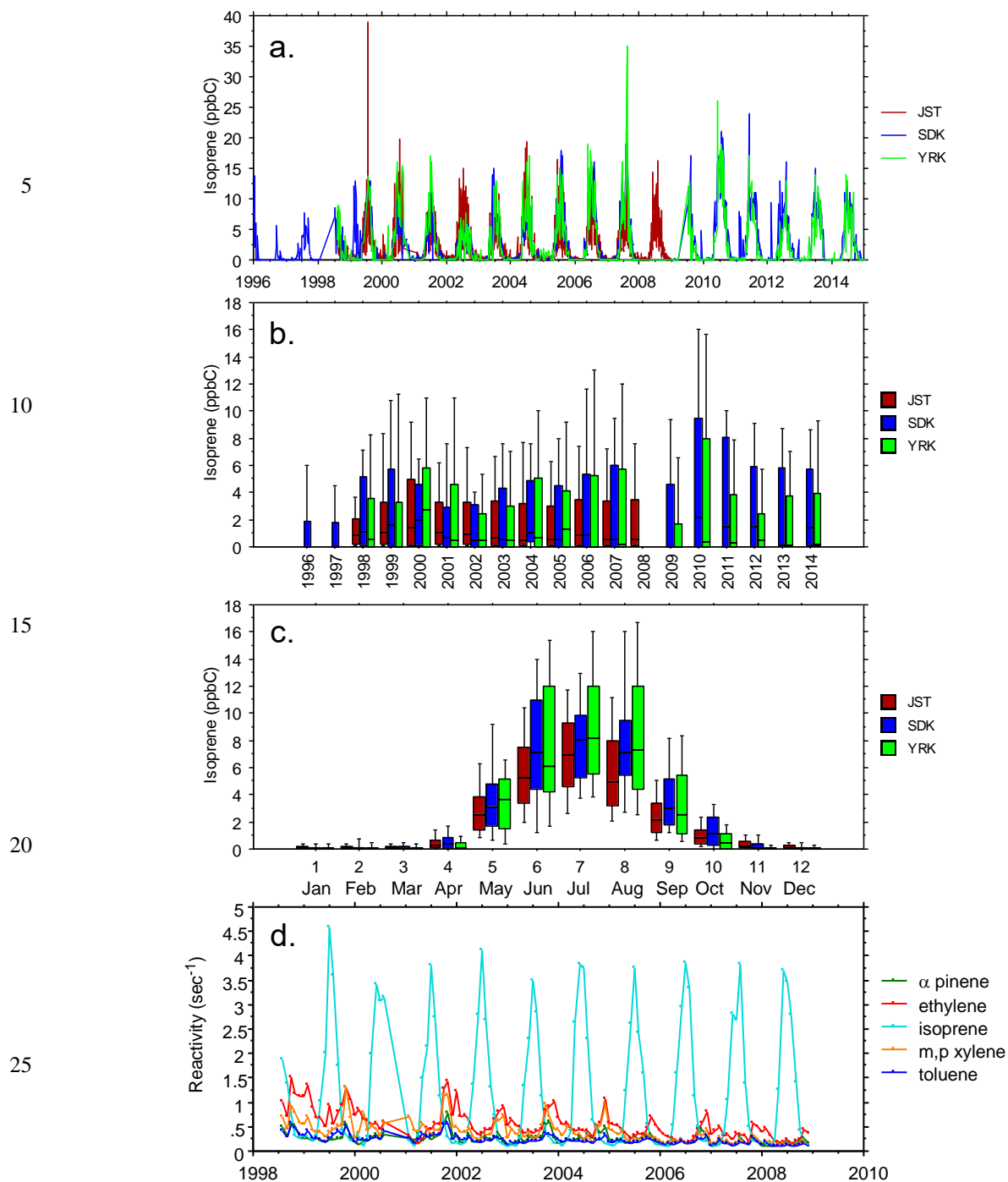
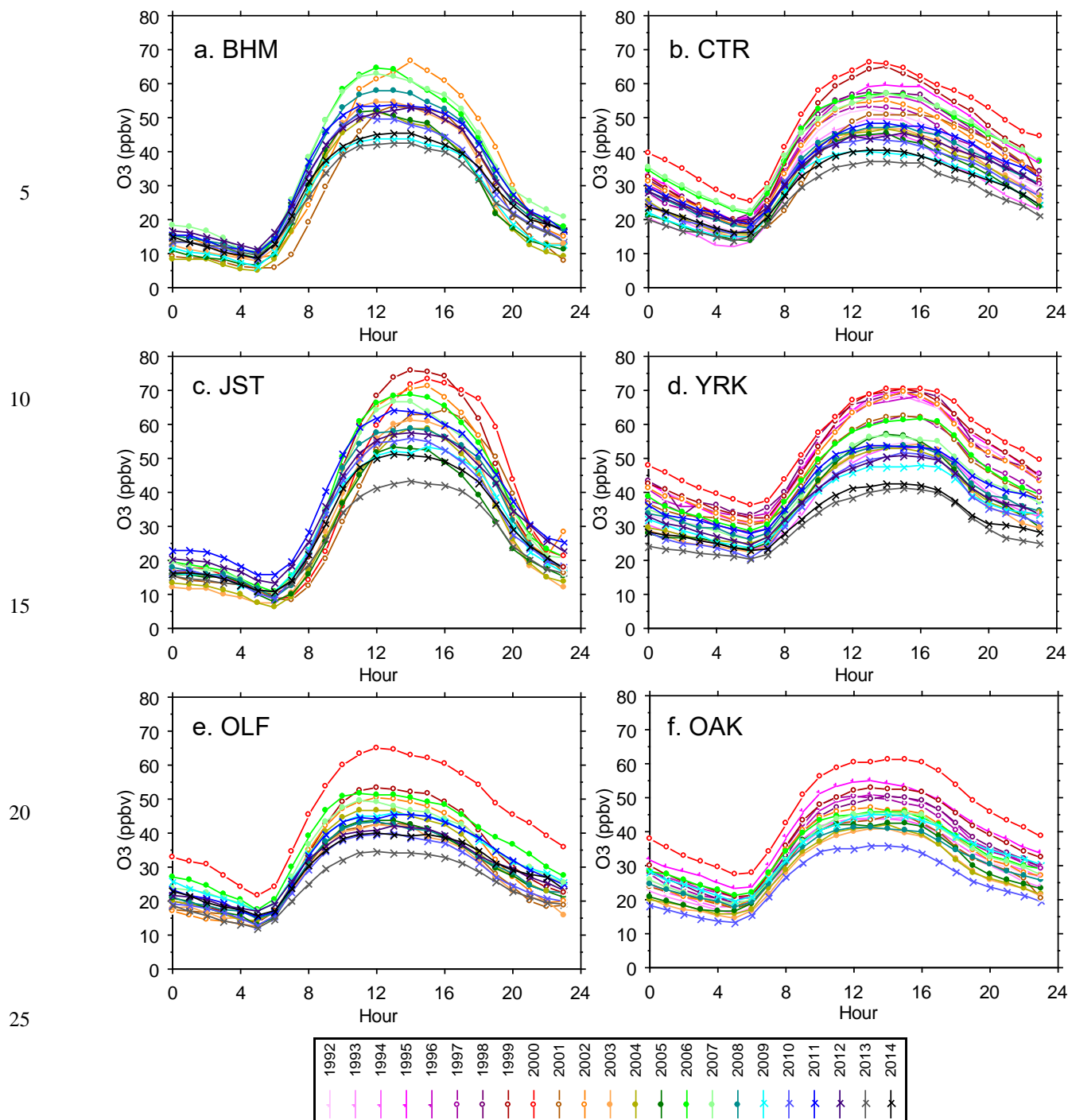


Figure 6. (a) Daily-average isoprene mixing ratios vs. date, (b) statistical distributions of daily-average isoprene mixing ratios vs. year, (c) statistical distributions of daily-average isoprene mixing ratios vs. month, and (d) JST OH reactivity of isoprene and other compounds. Samples were obtained every day at JST and once every six days at YRK and SDK (Blanchard et al., 2010). Distributions indicate the 10<sup>th</sup>, 25<sup>th</sup>, 50<sup>th</sup>, 75<sup>th</sup>, and 90<sup>th</sup> percentiles. OH reactivity is the product of concentration and rate constant,  $k_{OH}$ .



30 **Figure 7. Average O<sub>3</sub> mixing ratios vs. hour, by year. Each data point is the mean of all hourly measurements during June through August. Sites at PNS and GFP (not shown) exhibit similar diurnal profiles and trends (sampling at those sites ended after 2009 and 2012, respectively). Standard errors of the means are 0.3 – 4 ppbv, ~2% of mean O<sub>3</sub> mixing ratios.**

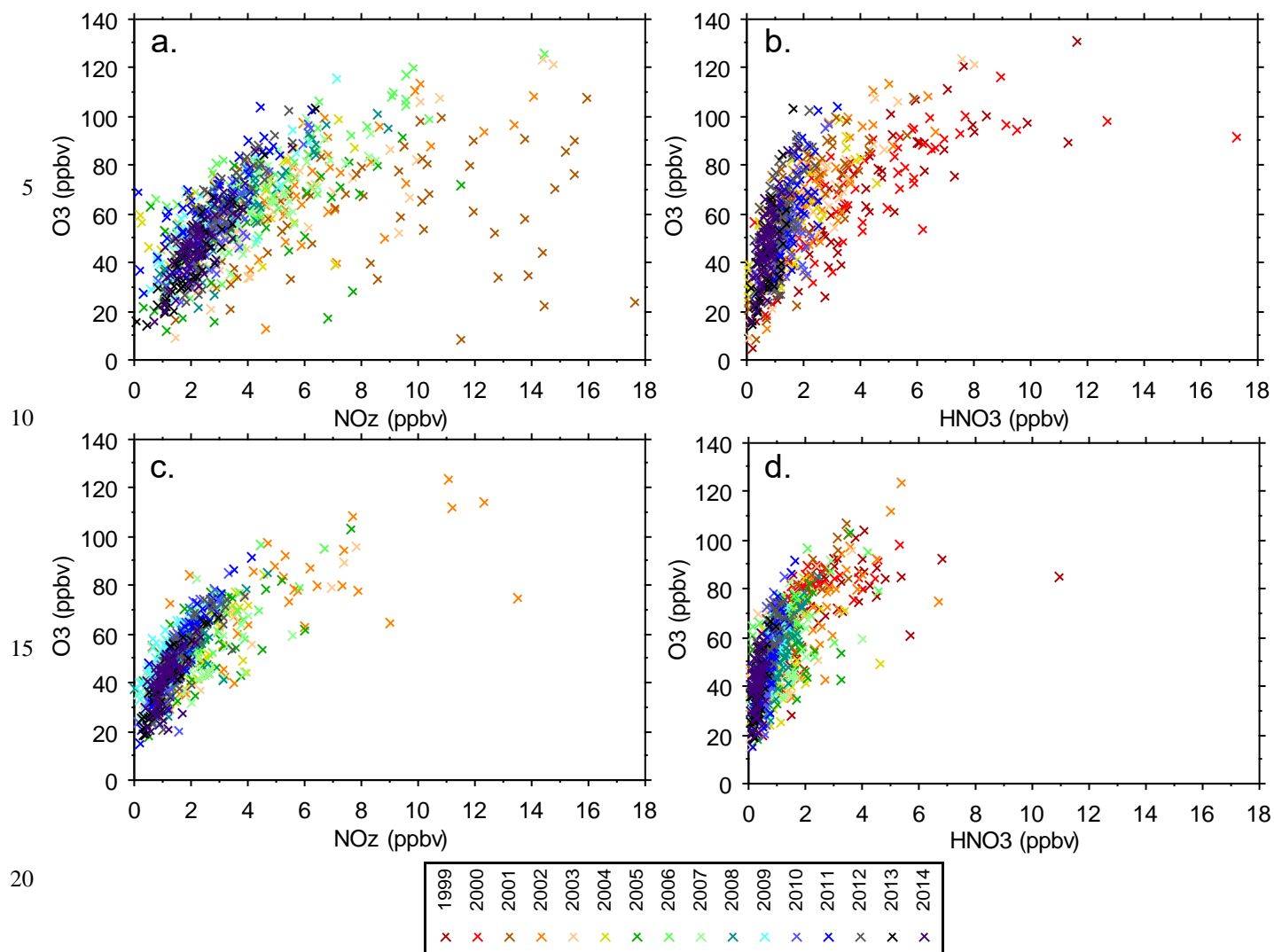
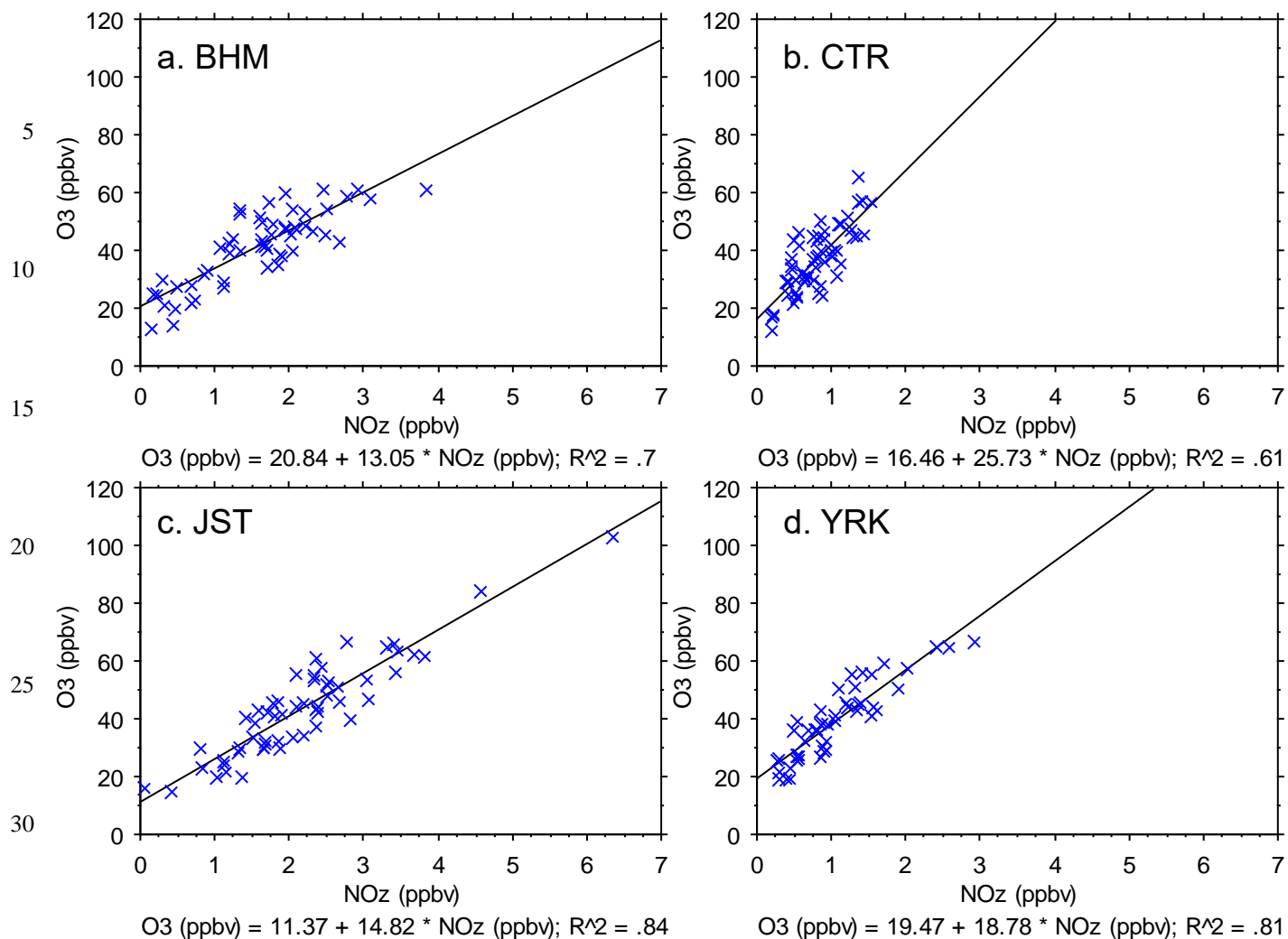


Figure 8. (a) O<sub>3</sub> vs. NO<sub>z</sub> at JST; (b) O<sub>3</sub> vs. HNO<sub>3</sub> at JST; (c) O<sub>3</sub> vs. NO<sub>z</sub> at YRK; and (d) O<sub>3</sub> vs. HNO<sub>3</sub> at YRK. Each point is the 2 – 3 p.m. hourly average on one day, limited to days in June or July and delineated by year. The 2001 and 2002 NO<sub>z</sub> data may be biased high due to lower NO<sub>2</sub> mixing ratios obtained by the instrumentation used at that time (Figure S2).



35 **Figure 9.** O<sub>3</sub> vs. NO<sub>z</sub> during June and July, 2013. Each point is the 2 – 3 p.m. hourly average on one day. The data were selected to represent the approximate mid-point of the mid-day O<sub>3</sub> maxima and to span a period around the summer solstice (- ~20 days, + ~40 days) when solar radiation is highest on average. The regression slopes are interpreted as an indicator of observed OPE, and show higher rural than urban values: BHM =  $13.05 \pm 1.19$  ppbv ppbv<sup>-1</sup>, JST =  $14.82 \pm 0.88$  ppbv ppbv<sup>-1</sup>, YRK =  $18.78 \pm 1.38$  ppbv ppbv<sup>-1</sup>, CTR =  $25.73 \pm 2.76$  ppbv ppbv<sup>-1</sup>. Corresponding regression slopes for O<sub>x</sub> vs. NO<sub>z</sub> are: BHM =  $12.00 \pm 1.16$  ppbv ppbv<sup>-1</sup>, JST =  $13.88 \pm 0.93$  ppbv ppbv<sup>-1</sup>, YRK =  $18.85 \pm 1.37$  ppbv ppbv<sup>-1</sup>, CTR =  $25.79 \pm 2.79$  ppbv ppbv<sup>-1</sup>.

40



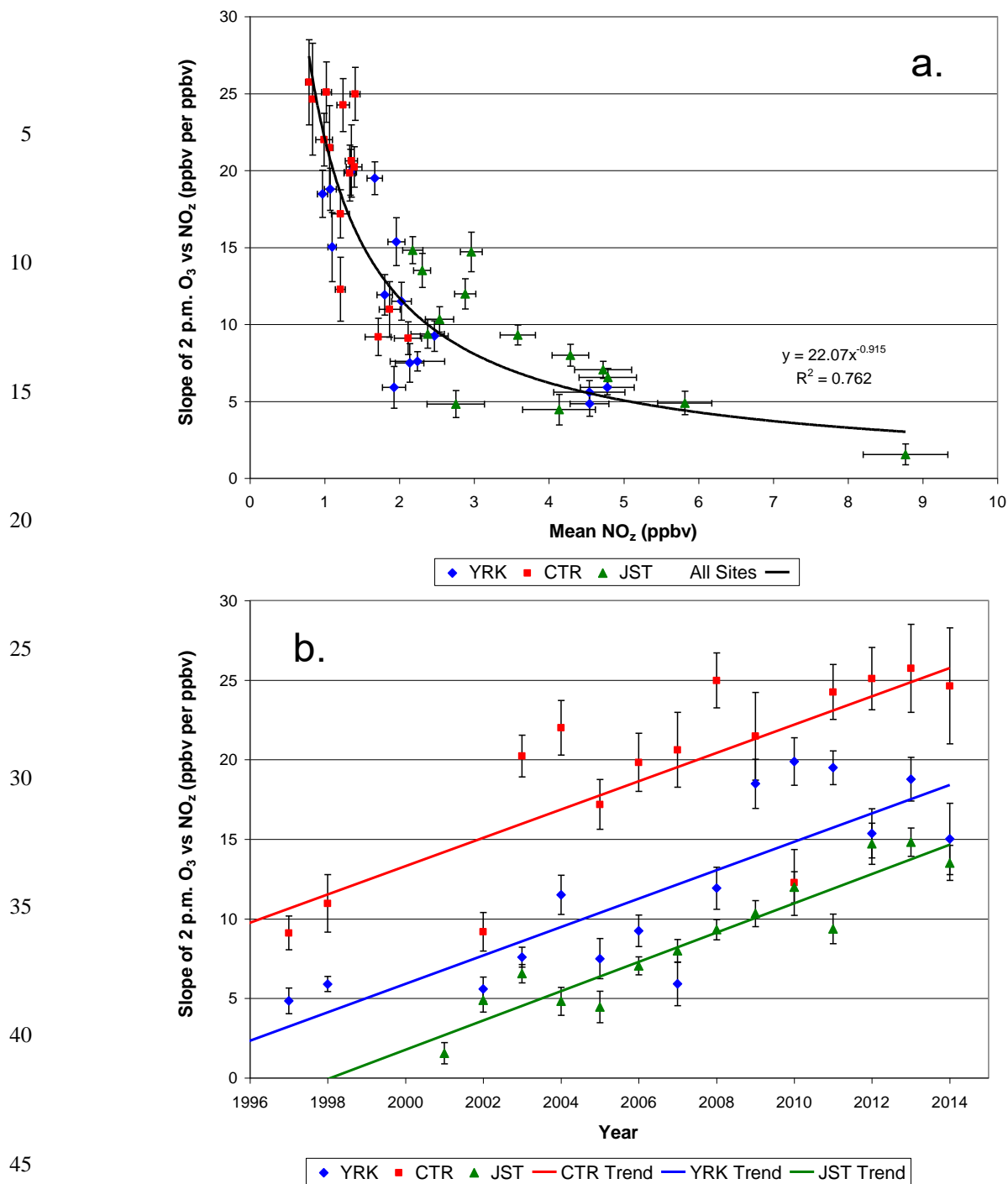


Figure 10. (a) Summer observed OPE at CTR, JST, and YRK computed as slope of daily (2 p.m.) O<sub>3</sub> and NO<sub>2</sub> vs. mean (2 p.m.) NO<sub>2</sub> mixing ratios, and (b) summer observed OPE vs. year. NO<sub>2</sub> data were not available for 1999 through 2001. Vertical and horizontal error bars are one standard error of the regression slopes and one standard error of the NO<sub>2</sub> means, respectively. Mean NO<sub>2</sub> measurement uncertainty is estimated as 0.2 ppbv (1 sigma).